Lipopolysaccharide suppresses activation of the tuberomammillary histaminergic system concomitant with behavior: a novel target of immune-sensory pathways

Ronald P.A. Gaykema, **Su-Mi Park**, **Christopher R. McKibbin**, and **Lisa E. Goehler**
Program in Sensory and Systems Neuroscience, Department of Psychology, University of Virginia, Charlottesville VA, 22904

Abstract

Infection and inflammation strongly inhibit a variety of behaviors, including exploration, social interaction, and food intake. The mechanisms that underlie sickness behavior remain elusive, but appear to involve fatigue and a state of hypo-arousal. Because histaminergic neurons in the ventral tuberomammillary nucleus of the hypothalamus (VTM) play a crucial role in the mediation of alertness and behavioral arousal, we investigated whether the histaminergic system represents a target for immune activation and, if so, whether modulation by ascending medullary immune-sensitive projections represents a possible mechanism. Rats were injected intraperitoneally with either the pro-inflammatory stimulus lipopolysaccharide (LPS) or saline, exposed to one of various behavioral tests that would induce motivated behavior (exploration, play behavior, social interaction, sweetened milk consumption). Upon sacrifice, brains were processed for c-Fos and histidine decarboxylase immunoreactivity. LPS treatment reduced behavioral activity and blocked behavioral testassociated c-Fos induction in histaminergic neurons of the VTM. These effects of LPS were prevented by prior inactivation of the caudal medullary dorsal vagal complex (DVC) with a local anesthetic. To determine whether LPS-responsive brainstem projection neurons might provide a link from the DVC to the VTM, the tracer Fluorogold was iontophoresed into the VTM a week prior to experiment. Retrogradely labeled neurons that expressed c-Fos in response to LPS treatment included catecholaminergic neurons within the nucleus of the solitary tract and ventrolateral medulla. These findings support the hypothesis that the histaminergic system represents an important component in the neurocircuitry relevant for sickness behavior that is linked to ascending pathways originating in the lower brainstem.

Keywords

arousal; sickness behavior; hypothalamus; dorsal vagal complex; dopamine-beta-hydroxylase; c-fos

Converging lines of evidence strongly implicate histamine in the mammalian brain in behavioral arousal, wakefulness, metabolic homeostasis, and learning (Haas and Panula, 2003). The activity of the histaminergic neurons in the ventral tuberomammillary nucleus (VTM) is strongly and positively correlated with an alert waking state and behavioral activity,

and remains low during slow wave sleep (Takahashi et al., 2006). Studies using transgenic mice lacking the L-HDC gene (Parmentier et al., 2002) or lacking the histamine H_1 receptor (Inoue et al., 1996, Huang et al., 2001) show impaired arousal and deficit in sustained waking during behavioral challenges, and suggest that an intact functional histaminergic drive is required for sustained arousal and adequate goal-oriented behavioral activity. Similarly, pharmacological inhibition of the posterior hypothalamus (Lin et al., 1989) shows a critical role for this region in adequate behavioral arousal and motivational drive. In addition, recent findings point to a mediating role for the histaminergic system, as these show a close temporal relationship between activation of histaminergic neurons and expectant behavior of food-entrained rats alerted prior to the onset of feeding upon delivery of food (Valdes et al., 2005). Taken together these findings implicate the histaminergic system in generating arousal states necessary for behavior.

Infections and inflammation produce marked effects on brain function and notably suppress behavioral activity. The ensuing sickness behavior is marked by fatigue, lethargy, and a general loss of motivational drive. Although such changes derive from a rearrangement of motivational state and are considered adaptive for the sick animal (Hart, 1988,Dantzer 2001), little is yet known about the mechanisms and neuronal systems involved, beyond brain regions that show marked activation upon inflammatory challenge with bacterial lipopolysaccharide (LPS) or the cytokine interleukin-1 (IL-1). The constellation of brain regions responding to immune activation (e.g. evidenced by induction of neuronal activation markers, such as c-Fos) includes most components of primary viscerosensory and central autonomic network nuclei (Elmquist et al., 1996; Ericsson et al., 1994; Konsman et al., 1999). Primary viscerosensory pathways originating in the caudal brainstem that respond to LPS and IL-1 project heavily to the hypothalamus, where they play a critical role in hypothalamus-pituitary-adrenal axis responses to systemic inflammation (Ericsson et al., 1994, 1997; Buller et al., 2001; Gaykema et al., 2007). These medullary projections to the hypothalamus are overwhelmingly catecholaminergic (Ericsson et al., 1994; Gaykema et al. 2007). A role for immune-sensitive brainstem projections in behavioral responses to inflammation is supported by the demonstration that inactivation (using a local anesthetic) of the dorsal vagal complex, a major source of ascending immune-sensitive pathways, prevented the induction of c-Fos protein in central autonomic brain regions, as well as the suppression of social behavior normally exhibited following LPS challenge (Marvel et al. 2004).

The constellation of brain regions activated by immune challenge reported so far does not include the ventral tuberomammillary nucleus (Miklos and Kovacs, 2003). However, as discussed above, because the activity of histaminergic neurons is not only closely tied to the level of alertness and vigilance (Takahashi et al., 2006), but disruption of normal histaminergic function consistently impairs these behavioral attributes (Inoue et al., 1996; Parmentier et al., 2002), these neurons may nevertheless contribute a critical link to the neurocircuitry that mediates behavioral symptoms associated with immune activation. In particular, neurovegetative symptoms, such as increased somnolence, lethargy, fatigue, psychomotor retardation (see Raison and Miller, 2003) may derive from impairments in histaminergic transmission.

Thus far, effects of systemic inflammatory challenge on the histaminergic system have received limited attention. As noted above, challenge with the proinflammatory stimulus LPS does not induce c-Fos protein in the VTM (Miklos and Kovacs, 2003). Rather, considering the inhibitory direction of behavioral changes characteristic in sickness, inflammatory stimuli may suppress, rather than enhance, the activity of neuronal populations that mediate or support arousal, vigilance, and the engagement in motivated behavior. Because the histaminergic system plays a critical role in waking, alertness, and behavioral arousal (Haas and Panula, 2003; Lin, 2000), this system may well function to mediate central adjustments that ultimately lead to the

manifestations of the behavioral (e.g., psychomotor and motivational) dimensions of the sickness syndrome. To test this possibility, we evaluated, by means of c-Fos expression, the activation of histaminergic neurons in behaviorally aroused rats that were challenged either with LPS or saline prior to testing. In addition, because we have previously shown that inactivation of the dorsal vagal complex (DVC) prevents social withdrawal behavioral seen following LPS treatment (Marvel et al., 2004), we assessed whether the effects of LPS challenge on the neuronal activity in the histaminergic neurons and exploratory behavior also depends on the integrity of the DVC. Finally, to explore potential anatomical links between brainstem and caudal hypothalamus that may modulate histaminergic neurons in the context of systemic inflammatory challenge, we investigated the distribution of LPS-responsive input to the ventral tuberomammillary nucleus.

EXPERIMENTAL PROCEDURES

Animals

The experiments involved 95 male Sprague-Dawley rats (Taconic Laboratories, Germantown, NY, USA) with initial body weights of 250–350 g, except for 17 acquired at a juvenile age with 100-120 g body weight. The adult rats were housed in pairs and the juveniles groups of four in propylene boxes on a barrier cage rack (Allentown, Caging Smart Bio-Pak, Allentown, NJ, USA) in a temperature and humidity controlled room. After at least one week of habituation upon arrival, rats assigned to the social interaction and sweetened milk/water consumption tests were singly housed one day before the start of the procedures. The rats were maintained on a 12-hour light-dark cycle (lights on at 7:00 AM) with free access to Purina Rat Chow #R001 and water. All animals were handled daily for at least one week prior to the experiments, to habituate them to the procedures and minimize stress reactions to cage displacement and the handling, which in the last three days prior to experiment also involved brief restraint in a towel while receiving a mock injection. All procedures were in accordance with the National Institute of Health Guidelines for the Care and Use of Laboratory Animals (NIH Publications No. 80-23; revised 1996) and were in accordance with protocols approved by the University of Virginia Animal Care and Use Committee. Every attempt was made to minimize the number of animals used in these studies and to limit their distress and potential suffering.

Pro-inflammatory challenge

During at least 3 days prior to the injections, all rats were gently handled and briefly restrained in a towel to receive a mock injection with a blunt end of a plastic syringe placed on the abdomen in order to habituate the animals to this procedure and minimize possible stress. The inflammatory stimulus LPS (serotype 0111:B4; derived from *Escherichia coli*; Sigma, St Louis, L-2013) was dissolved in sterile pyrogen-free saline (0.9% NaCl). Rats were injected intraperitoneally (i.p.) with either LPS (0.1 mg/kg) or equivolume sterile saline, both at a volume of 1 ml/kg, and immediately returned to their home cage. The injections were given between 10:00 and 12:00 h. The rats were then subjected to one of the behavioral experiments 90 or 120 minutes later as described below, or remained their home cage, and then sacrificed by perfusion fixation one hour after the behavioral testing. The home cage controls, as well as those receiving the retrograde tracer Fluorogold, remained undisturbed in their home cages during the entire period of 150 minutes before sacrifice.

Behavioral procedures

All behavioral experiments were carried out between 12:00 and 14:00 h. The order of animals tested was counterbalanced according to experimental group, in each experiment. For those experiments that involved transport to an adjacent room, the animals were habituated to the transport and novel environment by duplicating the transport procedure beginning three days prior to behavioral testing. The animals were allowed to remain in the procedure room for

approximately 2 h before being returned to the colony room. On the day of the experiment, the animals were transported to procedure room 1 h prior to the beginning of the experiment. This habituation protocol was undertaken to reduce novelty and arousal, and thus likely c-Fos induction, related to transport.

Exploratory behavior—Twenty four rats were divided into two groups, one group to be tested on the elevated plus maze (EPM, n = 14), the other to remain in their home cage in the colony room for the entire time (n = 10). The fourteen rats in the behavior test group were transferred in their cages to the adjacent experiment room one hour before testing (30 min after receiving the injections of LPS or saline). This time point was chosen to minimize c-Fos induction due to transport to the procedure room. Between 90–100 minutes after i.p. injection, each rat from the test group was placed in the center of the elevated plus maze and allowed to explore the maze for 5 minutes. The behavior was recorded using a digital camcorder positioned above the maze. Exploratory behavior was assessed by numbers of entries into closed, open, and all arms during the 5 minutes of testing. In addition, the occurrence and frequency of immobility was scored as a measure of sickness behavior. After the test, the rats were returned to their home cage and sacrificed by perfusion fixation one hour later.

Home cage control group—Ten rats assigned as home cage controls received the intraperitoneal LPS and saline injections in the same time window as the EPM group described above, after which they were left undisturbed in the home cage prior to sacrifice by perfusion fixation, in order to prevent behavioral arousal to allow the assessment of c-Fos induction in the VTM due to LPS challenge. The time lapse in between injection and sacrifice was kept the same, i.e., 150–160 minutes, to ascertain that sacrifice occurred at the same time points as the rats in the EPM group.

Play behavior—In this experiment, juvenile rats were used and were trained over a period of 7–10 days to engage in playful behavior within the context of a Y maze. Twelve juvenile rats (100–120 g) were initially housed in groups of four. This test is a modification on studies by Panksepp and colleagues (Burgdorf and Panksepp, 2001). During the first week of training they were transferred daily to the testing room and allowed one hour of accommodation before testing. Groups of 4 cage mates were placed in a Y maze (3 arms joining in the center at 120 degrees angle) for 5 minutes. The experimenter used one hand at the end of one arm to administer tactile stimulation ("tickling") to the rats upon approach and voluntary contact or sniffing of the hand. The next two days, the procedure was repeated, while the cage mates were gradually separated, by first being housed in pairs, and thereafter single-housed. During this period, the groups of 4 rats that were separated from each other were reunited in the Y maze for 5 minutes, provoking social interaction including "rough-and-tumble" play behavior. Both the maze and the experimenter's hand were then conditioned stimuli for social interaction. The following week, each of the singly housed young rats was placed in the Y maze alone, upon which the animal oriented towards the experimenter's hand at the end of the maze arm as the sole social stimulus. This test condition allowed the experimenter to administer tactile stimulation including tickling and occasional pinning the rat on its back), which was actively sought after by the now single-housed animals. After two successive test days to record baseline behavior, the young/adolescent rats (170–200 g) were injected with either LPS or saline on the third day between 10:00 AM and noon. One hundred minutes later, they were placed in the Y maze to record play behavior for 2 minutes, after which they were returned to their home cage. The behavior was recorded with a digital camcorder. One hour after the test the rats were sacrificed by perfusion-fixation.

Social interaction—Ten male adult rats (350–370 grams) and 5 juveniles (100–150 g) were used in this test. The rats were individually housed one week prior to testing. On the days of

testing the rats in their home cages were transported to the adjacent behavioral testing room 1 hour prior to testing. The test was performed as previously described (Marvel et al. 2004). Baseline social interactions were measured on two consecutive days, followed by the experiment on the third day on which half of the adults received i.p. injections of LPS and the other half sterile saline 2 hours prior. Each rat had an encounter with 3 different juveniles on the three successive tests. The behavior was recorded with a digital camcorder. One hour after the test the rats were anesthetized with i.p. pentobarbital (60 mg/kg) for perfusion-fixation.

Sweetened milk intake—Twelve male adult rats (300–330 grams) were separated and singly housed and, on 7 consecutive days, received 30 ml of a sweetened milk solution (diluted with equi-volume water) for 30 minutes at a specific time (between 11:00 AM and 1:00 PM), during which the original water bottle was temporarily removed. At all other times water and food was kept available *ad libitum* to motivate the rats based on the positive rewarding aspects of the taste, rather than by hunger or thirst due to food or water deprivation. The rats increased the consumption of the sweetened milk solution over the successive days, and the total intake reached a plateau after 5 days. The baseline intake was calculated from the average intake on the 6th and 7th day. The following day, rats received either i.p. saline or LPS challenge 2 hours prior to the 30-minute presentation of the sweetened milk solution, and were anesthetized with i.p. pentobarbital (60 mg/kg) 60 minutes after the time point on which the milk solution was removed. Twelve other male rats (similar body weights) served as a control group and underwent the same procedure, including single housing and switching of drink bottles on successive days, except they were offered water instead of sweetened milk solution throughout the entire procedure.

Dorsal vagal complex (DVC) inactivation

Using a reversible inactivation technique, we have previously shown that the caudal brainstem DVC contributes to inhibition of behavior, and induction of c-Fos protein in autonomic brain regions (Marvel et al. 2004). This technique produces minimal brain damage and in non immune-challenged animals has no effect on social behavior. In LPS-challenged (i.p.) animals DVC inactivation normalizes behavior, and there is no effect on e.g. respiration, that would suggest autonomic impairment. Indeed, the technique is used explicitly to avoid autonomic effects of structural lesions in critical viscerosensory relay regions (e.g. Williams & McGaugh, 1993). Co-injection of the tracer fluorogold has shown the injection to be limited to the caudal NTS and area postrema (Marvel et al. 2004), the sensory components of the DVC. We used this technique to determine whether the dorsal vagal complex contributes to the effects of LPS challenge on tuberomammillary c-Fos induction.

Cannula implantation—For this experiment, a group of 20 rats received double-barrel stainless steel guide cannulae (26 gauge, 1.5 mm distance, Plastics One, Roanoke VA) were aimed at a position of 1 mm above the center of the medial NTS in both hemispheres as described (Marvel et al., 2004). Briefly, rats were anesthetized as described above and their heads placed into a stereotaxic device (David Kopf). Two self-tapping skull screws were placed for anchoring the guide cannula. The stainless steel guide cannulae were then implanted bilaterally 1mm above the site of injection (NTS) according to the following coordinates: 13.6 mm caudal from bregma, 0.75 mm lateral from the midline and 6.5 mm below the skull surface (Paxinos and Watson, 1998). After implantation, each cannula was cemented in place using dental acrylic cement with the inclusion of the skull screws, the cement allowed to dry, after which the skin was closed with wound clips. Stylets were placed inside the guide cannula to prevent obstruction. During the following recovery period, the animals were housed individually and handled to minimize non-specific stress. The rats that received cannula implantation were allowed 10–14 days of recovery prior to testing.

Infusion and behavioral testing—During the 4 days prior the animals were handled and mildly restrained to habituate to the infusion procedure. The rats were randomly assigned to either of the treatment groups according to a two-by-two factorial design (DVC: bupivacaine/saline; i.p. LPS/saline). On the day of the experiment the rats were transported in their home cage to the test room. The animals were mildly restrained by hand and beveled injector cannulae (33-gauge, Plastics One) connected to Hamilton 10 µl syringes via a PE20 tubing were inserted that extended 1mm below tip of the guide cannula to extend bilaterally into the DVC. Thereafter, an automated syringe pump (Kd-Scientific) slowly infused the nerve block bupivacaine (0.5%, Marcain, Abbot Laboratories, North Chicago) or sterile saline at a rate of 0.1 µl over a 5 min period (final volume administered: 0.5 µl). All injections contained a small amount (0.01%) of the fluorescent tracer Flurogold for the purposes of verifying the location of the cannulae, and determining the likely spread of the infused substances. After completion of the infusion, the injectors were left in place for 2 minutes before removal after which the animals received an i.p. injection of either LPS or sterile saline, and were then returned to their home cage, where they were observed for signs of illness or distress. Ninety minutes following LPS or saline injection, the animals were tested on the elevated plus maze (described above in "exploratory behavior"), and sacrificed for perfusion fixation one hour later as described above.

Retrograde neural tracing with Fluorogold

Twelve adult rats (290−330 g) were sedated with medetomidine HCl (Dormitor, Pfizer Animal Health, Exton, PA; 0.06 ml i.m.) and ketamine (Ketaset, Fort Dodge Animal Health, Fort Dodge, IA; 0.1 ml s.c.) and received 10 ml saline s.c. to prevent dehydration. The rats were mounted in a stereotaxic frame with the skull surface in a flat position and general anesthesia was maintained on isoflurane delivered at 1% with oxygen flow (1 liter/min). After exposing the skull surface and drilling a bur hole, Fluorogold (Fluorochrome, Denver, CO; 5% in sterile saline) was backfilled in beveled glass micropipettes, and the tip was moved to the following coordinates: −4.3 mm caudal to bregma, 1.4 mm lateral to midline, and 9.0 mm ventral from the brain surface with the skull surface in a flat position (Paxinos and Watson, 1998). Fluorogold was delivered by iontophoresis by a current of 2 µA (7s on/off cycle for 20 minutes) from a Midgard[TM] Precision Current Source (Stoelting, Wood Dale, IL). The tip was left in place for an additional 5 minutes before retraction to minimize diffusion along the track. After the wound was sutured, atipamezole HCl (Antisedan, Pfizer Animal Health, Exton, PA; 0.06 ml/kg i.m.) was injected i.m. to reverse medetomedine-induced sedation, as well as the analgesic ketoprofen (0.1 mg s.c.) and the antibiotic enrofloxacin (Baytril, Bayer; 2.27%, 0.2 ml s.c.). Upon return to their home cages, the rats recovered for 10−14 days. Subsequently, they received intraperitoneal injections of LPS (0.1 mg/kg) or sterile saline and were sacrificed 2 h later by perfusion fixation.

Perfusion fixation

The animals were deeply anesthetized with an injection of pentobarbitol (60 mg/kg), and then perfused through the aorta with saline (100 ml) followed by fixative (freshly prepared 4% paraformaldehyde in 0.1 M phosphate buffer with 15% saturated picric acid, pH 7.4). The brains were subsequently removed and post-fixed in the same fixative overnight, stored in 0.1 M phosphate buffer containing 0.1% sodium azide (PB-azide), blocked into 4 parts and sectioned in the coronal plane on a Vibratome in sections at a thickness of 50µm. Brain sections were collected serially in one-in-six sets and stored in 0.1 M PB-azide in six-well plates at 4 °C prior to the immunohistochemical staining procedures.

Immunohistochemical procedures

Because the different sets of brains were not processed simultaneously, as this study involved different experiments, care was taken that all series of sections were processed in the same

fashion, with identical dilutions and incubation times in each batch. Brain sections derived from each experimental procedure, however, were collectively run up to avoid intra-experimental variability in staining. The primary antibodies used were from the same batch throughout the study, to avoid batch-to-batch variability in staining quality. All sets of brain sections were rinsed between incubation steps in phosphate buffered (0.01 M, pH 7,4) saline (PBS). Solutions for pre-incubation and for primary and secondary antibodies consisted of PBS to which Triton X-100 (0.5%), normal goat serum (Jackson Immunoresearch, 5%), and sodium azide (0.1%) were added. For purpose of reducing nonspecific staining, sections were treated in 0.1% sodium borohydrate in PBS for 10 minutes and in a mixture of hydrogen peroxide (0.3%) and sodium azide (0.1%) in PBS for 30 minutes, and transferred to a pre-incubation solution containing normal goat serum (5%) and Fab' fragment of goat anti-rat IgG (1:500) for an overnight incubation. The primary antibodies used in this study include: rabbit anti c-Fos (Ab5, Oncogene, Cambridge, MA), rabbit anti-Fluorogold (AB153, Chemicon, Temecula, CA), rabbit anti-histidine decarboxylase (HDC; #P4211, CURE/Digestive Diseases Research Center, Los Angeles, CA), mouse monoclonal anti-dopamine beta-hydroxylase (DBH; MAB308, Chemicon), rabbit anti-phenylethanolamine-N-methyltransferase (PNMT, #22572, Immunostar, Hudson, WI), and rabbit anti-adenosine deaminase (anti-ADA, AB176, Chemicon). ADA, like HDC is specifically contained in histaminergic neurons in the ventral tuberomammillary region, and anti-ADA antibodies are alternatively used to stain the histaminergic cell groups (Ko et al., 2003). Here, we identified histaminergic neurons by their ADA immunoreactivity in combination with staining of DBH- and PNMT-immunoreactive fibers and terminals. All biotin- and fluorescent label-conjugated secondary antibodies (goat anti-rabbit IgG, goat anti-mouse IgG) with minimal crossreactivity to other hosts' immunoglobulins were purchased from Jackson Immunoresearch (West Grove, PA). Immuno-peroxidase labeling was accomplished using the avidin-biotin-peroxidase complex (ABC, PK-6100) Elite kit from Vector Laboratories (Burlingame, CA). Incubations that lasted for one overnight or longer were carried out in refrigerated environment under gentle agitation on a rotating platform.

c-Fos immunohistochemistry—The first and fourth series of sections through the posterior hypothalamus were stained for c-Fos, immunoreactivity as previously described (Goehler et al., 2005). These sections were incubated in anti-Fos (1:50,000 for 3 days), in biotinylated goat anti-rabbit IgG (Jackson Immunoresearch, 1:1000, overnight), followed by the ABC kit (Vector, 1:500, overnight). Staining for c-Fos immunoreactivity was completed using nickel-enhanced 3,3'-diaminobenzidine (DAB, 0.02%, nickelous ammonium sulfate 0.15%) in Tris-HCl (0.05M, pH 7.6) yielding a black reaction product that was accomplished with a modified glucose oxidase protocol to generate hydrogen peroxide in the incubation solution.

Double c-Fos and histidine decarboxylase immunostaining—Additional series (the second and fifth sets) of sections through the posterior hypothalamus (including the tuberomammillary region) were stained for c-Fos as described above and subsequently processed for histidine decarboxylase (HDC) immunoreactivity. After immersion in 0.3% hydrogen peroxide for 30 min, the sections were successively incubated in solutions containing rabbit anti-HDC 1:2,000 overnight), biotinylated goat anti-rabbit IgG (1:1,000), and ABC kit (1:500), and finally reacted with DAB (0.04%) yielding a reddish-brown cytoplasmic staining. After staining, all sections were mounted, dehydrated, and coverslipped on gelatin-coated microscope slides.

Double and triple immunostaining of c-Fos, Fluorogold, and dopamine beta-hydroxylase—One set of sections through the entire rostrocaudal extent of the brains from rats from the retrograde tracing experiment were stained for c-Fos immunoreactivity yielding

a black nuclear staining as described above, followed by a second immunoperoxidase staining procedure to stain the retrogradely transported Fluorogold (FG). Following c-Fos immunostaining, sections were incubated in rabbit anti-FG (1:10,000 overnight), biotinylated goat anti-rabbit IgG (1:500), and ABC (Vector, 1:500), and finally reacted with DAB (0.04%) yielding a reddish-brown staining. To identify the neurochemical phenotype of projection neurons in the brainstem, the second and fifth sets of sections through the pons and medulla were used for triple immunolabeling of c-Fos, FG, and dopamine β-hydroxylase (DBH), the noradrenaline synthesizing enzyme. First, the sections were stained for c-Fos immunoreactivity using the immunoperoxidase procedure with nickel-DAB to yield an intense black reaction product (see above) followed by double immunofluorescence labeling of FG and DBH. Although FG has fluorescent properties, its signal is not as strong as the other fluorescent dyes and fades quickly. The FG signal is dramatically amplified by this method. Sections were washed in PBS and incubated in rabbit anti-FG (1:10,000) overnight followed by Alexa Fluor 488 conjugated goat anti-rabbit IgG (Molecular Probes, 1:500) overnight. Lastly, sections were incubated in monoclonal mouse anti-DBH (Chemicon, 1:5,000) followed by by Alexa Fluor 546 conjugated goat anti-mouse IgG (Molecular Probes, 1:500). The sections were then rinsed in PBS, mounted on microscope slides, air-dried, and coverslipped in a PBS-glycerol (1:2) mixture.

Double Fluorogold and HDC immunostaining—An additional set of sections through the hypothalamus from brains of the rats that were received Fluorogold (FG) injections in the retrograde tracing experiment were processed for the localization of the tracer deposit in the injection site. The sections were first incubated in anti-FG antibody mixture followed by biotinylated goat anti-rabbit and ABC (as described above) and reacted with nickel-enhanced DAB to yield a black staining; followed by incubation in anti-HDC and repeated steps in the secondary antibody and ABC mixtures (as described above), after which they were reacted with regular DAB. The sections were then mounted, dehydrated and coverslipped in DPX mounting medium.

Double DBH/PNMT and ADA immunstaining—Two extra sets of sections through the hypothalamus were selected to stain for adenosine deaminase immunoreactivity, another specific marker for histaminergic neurons in the VTM, in conjunction with immunostaining for the catecholamine biosynthetic enzymes DBH in one and PNMT in the other set to visualize noradrenergic and adrenergic innervation in specific relationship to the histaminergic neurons. One set of sections was incubated in mouse anti-DBH (1:5,000, 48h), followed by biotinylated goat anti-mouse IgG (1:1,000, overnight) and ABC (1:500, overnight). In parallel, the other set was immersed in rabbit anti-PNMT (1:5,000) followed by biotinylated goat anti-rabbit IgG (1:1,000) and ABC. The immunolabeling for DBH and PNMT was visualized using nickel-enhanced DAB (as described above) to yield crisp black axonal branches, varicosities, and terminal boutons. Subsequently, both sets were incubated in rabbit anti-ADA (1:2,000, 2 days), biotinylated goat anti-rabbit, and ABC, and reacted in regular DAB to yield brown cytoplasmic staining. The sections were then mounted, dehydrated and coverslipped.

Microscopy and photography—All slides examined in an Olympus BX51 microscope equipped with bright-field as well as epi-fluoresence illumination. Images were captured with a Magnafire digital camera (Optronics, Goleta, CA), and analyzed with NIH Image software for counting the c-Fos-immunoreactive profiles. Photomicrographs were cropped, resized and adjusted in brightness and contrast in Adobe Photoshop CS2 (Adobe Systems, Mountain View, CA).

Semi-quantitative analysis of neuronal c-Fos expression

Two out of six sets (either the first and fourth, or second and fifth, which were 150 µm apart) of sections were combined for the semi-quantitative assessment of neuronal activation in the VTM. This region contains distinct clusters of histaminergic neurons that are concentrated near the ventral surface, labeled E1-E3 cell groups (Miklos and Kovacs, 2003), with additional cell clusters situated dorsomedially in the vicinity to the third ventricle (the medial E4 and E5 cell groups). In the semi-quantitative analyses in the sections double-stained for c-Fos and HDC, cell counts in these subgroups were combined to yield one total, as the induction of c-Fos occurred uniformly across all subgroups. The total counts were corrected for over-estimation using the method of Abercrombie (1946).

In the series with double staining for c-Fos and HDC, the relative activation of HDC-immunoreactive neurons was determined by counting c-Fos-HDC double-stained neurons that harbored both brown cytoplasmic and dark grey-black nuclear reaction products, as well as HDC-positive cell bodies that displayed a distinct unstained nucleus (thus labeled as c-Fos-negative), to determine the total number of HDC cells with visible nuclei and the proportion that was c-Fos-positive. Every third section through the ventral tuberomammillary region was included in the summation of the counts obtained from both hemispheres to obtain the cumulative numbers of double-labeled and singly HDC-stained neurons for each rat. The percentage of HDC-positive cells that were c-Fos-positive was then calculated as the proportion of the total number of HDC-positive neurons (c-Fos-positive and negative). When sets were stained for c-Fos only, portions of the ventral tuberomammillary areas were identified and outlined where characteristically dense clusters of magnocellular histaminergic neurons reside (Ericson et al., 1987; Senba et al., 1985). Here, a total of 4 sections per rat were used in which the anterior and mid-ventrolateral E2 (2 sections), the mid-ventral E3 (1 section) and the caudoventral E1 cell groups were outlined in both hemispheres. Cell counts were generated with the NIH Image software as described previously (Marvel et al., 2004), and summed across all 4 sections and hemispheres. The cell counts were corrected for sampling bias using the method of Abercrombie (1946), with the size of the cell nuclei used as reference.

The sets of brainstem sections processed for triple-labeling for c-Fos, FG, and DBH immunoreactivity were analyzed in a similar fashion, by alternating epifluoresence filters to count the FG-positive neurons labeled with the fluorophore Alexa Fluor 488 and those that were also DBH-positive (labeled with Alexa Fluor 546). Only those FG-labeled cells were included in the count that displayed a prominent nucleus in the plane of the section, in order to determine whether these cells displayed additional c-Fos immunoreactivity or not. Cells lacking a visible nucleus were not included in the counts. With the superimposed bright field illumination, the number of FG-labeled and FG-DBH double-labeled cells were determined that also exhibited a c-Fos-stained nucleus visible by the black immunoperoxidase reaction product. Brain sections throughout the rostrocaudal extent of the NTS and the VLM, as well as the locus coeruleus, were included. In each rat, the total number of single-, double-, and triple-labeled cells were determined by summation of counts from both hemispheres and from each third section used. From these totals, the fractions of FG-labeled neurons that were DBH-positive and of those that were c-Fos-positive were determined, as well as the fractions of FG-DBH-double labeled neurons that were c-Fos-positive. In the LPS-treated groups, but not the saline-treated group due to lack of c-Fos staining, we also determined the fraction of all FG-c-Fos-double labeled neurons encountered that were DBH-positive.

Statistical analysis

Behavioral data from the EPM exploration test (number of arm entries) were analyzed using analysis of variance (ANOVA). Behavioral data from the play test (numbers of arm runs) sweetened milk (grams ingested) and social interaction tests (duration of active social

engagement by the adult) were analyzed using two-way ANOVA with the i.p. challenge (saline *vs.* LPS) as the between-subject factor and with time of testing (pre-injection baseline and post-injection) as a within-subject factor. Exploration data from the DVC inactivation experiment were analyzed using two-way ANOVA, with i.p. treatment (LPS or saline) and DVC infusion (bupivacaine or saline) as between-subject factors. Post-hoc comparisons of individual group means were carried out by Fishers protected least significant difference test (LSD). Values of $p < 0.05$ were considered significant in all tests.

The effects of behavioral testing and LPS treatment on neuronal activation (cumulative counts of c-Fos-positive cells) and on the numbers of neurons double- or triple-labeled were analyzed, dependent on the number of independent variables, using one- or two-way ANOVA. The Bonferroni/Dunn test was used for post hoc comparison of differences between the experimental groups, with values of $p < .05$ considered the criterion for statistical significance. When counts were converted in percentages (double/triple-labeled cells) in order to compensate for larger variations of counts within groups (e.g., in the retrograde tracing experiments), nonparametric analyis was applied using the Mann-Whitney U test.

RESULTS

Behavioral effects of LPS treatment

In all four tests, LPS treatment had a strong inhibitory effect on the behavioral activity of the rats, including exploration, playful behavior and social interaction, as well as on the consumption of palatable food.

Exploration of a novel environment (elevated plus maze)—Rats placed on the center of the elevated plus maze initiated exploratory behavior consisting of entering (predominantly the closed and occasionally the open) arms, traversing to the ends of these arms and returning to the center. Other behaviors included scanning, head dips, and rearing (mostly in closed arms). Prior challenge with LPS reduced exploratory behavior as the number of total arm entries significantly decreased compared with the saline-treated rats (from 12 to 5 arm entries on average) as depicted in Fig. 1A. The LPS-treated rats generally exhibited a slower locomotion and assumed a "hunched" posture, and most of them also exhibited brief moments of immobility, which was not observed in the saline-treated rats. The ratio between open and closed arms, which is generally considered a measure for anxiety-like behavior, was not affected by treatment with LPS (not shown).

Play behavior—Upon placement in the center of the Y maze, the young rats displayed play solicitations consisting of runs through all arms, darting, and voluntary contacts and occasional nipping of the experimenter's hand that was kept at one arm end (in response to tactile stimulation by the experimenter to mimic rough-and-tumble play). The rats showed a consistent level of behavioral activity on the successive test days. On the experiment day, LPS treatment strongly reduced their active behavior, as reflected in the reduced number of maze arm entries (Fig. 1B, interaction test time × treatment $F(1,18) = 5.78$, $p = 0.027$). Although the rats were still predominantly present in the vicinity of the experimenter's hand, they displayed only limited playful behavior, but were not averse to manual contact.

Social interaction—The introduction of a conspecific juvenile into the experimental rat's home cage initiated social activity in the adult rat that includes close following of the juvenile, ano-genital sniffing, and direct physical interaction such as grooming as described previously (Marvel et al., 2004). LPS challenge inhibited this social activity reflected in the reduced amount of time spent by the experimental rats actively engaging with the juvenile (Fig 1C, interaction test time × treatment $F(1,16) = 6.56$, $p = 0.021$).

Sweetened milk intake—The rats in the sweetened milk group consumed between 11 and 21 grams of the diluted sweetened milk solution presented in their home cage on the 6th and 7th day, which amounts were used to calculate the baseline averages (15.8 +/− 1.4 grams). On the experimental day, the LPS- treated rats reduced their intake significantly (3.8 +/− 1.5 grams, range 0–9 grams), a 75% reduction relative to the saline-treated group, see Fig. 1D, interaction test time × treatment $F(1,16) = 11.81$, $p = 0.017$). The rats in the control group that received water, instead of sweetened milk, consumed little (range 0.4–3.4 g; average 1.5 +/− 0.5 g) during 30 min presentation of the drinking bottle, and LPS treatment further inhibited water intake (range 0.0–0.3 ml; average 0.1 +/− 0.1).

Modulation of histaminergic neuronal activity by LPS challenge

LPS challenge suppresses neuronal activation in the tuberomammillary region associated with behavioral testing—All four behavioral procedures were associated with strong c-Fos immunoreactivity in the histaminergic cell-rich regions of the VTM (Fig. 2A,C,D,E; Fig. 3), in a pattern identical to the distribution of histaminergic neurons, i.e., just above the ventral surface of the posterior hypothalamus and lining the lateral edges of the mammillary bodies. The tests in which the animals were removed from their home cage, i.e., EPM exploration and the play test in the Y maze, led to very strong induction of c-Fos immunoreactivity in the ventral subgroups of the VTM. Social interaction of adult rats with conspecific juveniles and consumption of sweetened milk solution, during which rats remained in the home cage, induced moderate levels of c-Fos in the VTM (Fig. 3). The induction of c-Fos appeared in similar intensity in the different subregions of the VTM. Little or no c-Fos staining was present in the VTM of rats that were left undisturbed in their home cage (Fig 2B, 3B). Similarly, very little c-Fos induction was seen in rats that were offered water-containing drinking bottles instead of sweetened milk (Fig 2F, 3F). In comparison with saline treatment, LPS challenge prior to the behavioral tests strongly reduced the number of c-Fos-immunoreactive profiles in the VTM associated with EPM exposure (Fig. 2A, 3A), play behavior (Fig. 2C, 3C), social interaction with a conspecific juvenile (Fig. 2D, 3D), and intake of sweetened milk solution (Fig. 2E, 3E). The low number of c-Fos immunoreactive profiles in the VTM of LPS-treated and behaviorally challenged rats was similar to that seen in the home cage controls that were kept undisturbed (Fig 2B, 3B) or were offered water (Fig. 2F, 3F).

Suppression of c-Fos in histaminergic neurons associated with behavioral testing in LPS-treated animals—Sections through the posterior hypothalamus from rats subjected to EPM exploration, and from those left undisturbed in their home cage were processed for identification of histaminergic neurons by peroxidase staining for histidine decarboxylase (HDC) immunoreactivity, as well as nuclear staining for c-Fos. HDC-positive somata were distributed in the VTM as previously reported (Ericson et al., 1987). In the home cage controls, little if any c-Fos immunoreactivity was present in the HDC-positive cells as these were devoid of any nuclear stain (Fig 4A). In contrast, rats that were engaged in exploration of the EPM showed abundant c-Fos-positive nuclear staining in the greater majority of HDC-positive cells (Fig 4B). However, following prior LPS treatment, little c-Fos staining was observed in the HDC-positive neurons in either rats that remained in the home cage (Fig. 4C) or that were placed on the EPM (Fig. 4D).

Semi-quantitative analysis revealed that EPM exposure dramatically increases c-Fos staining in HDC-positive neurons (approximately 80% of the total number of HDC-positive cells counted), whereas LPS treatment drastically diminished the EPM-associated c-Fos staining in the HDC neurons (Fig. 4E, test × treatment interaction, $F(1,20) = 49.61$, $p < 0.0001$). in such a way that little c-Fos was expressed by HDC neurons (apparent in approximately 10% of the

total counted) in either home cage and maze exploring groups after LPS treatment (Fig. 4E). No significant differences were seen in the total number of HDC-positive cell bodies (Fig. 4F).

Dorsal vagal complex inactivation counters suppression of behavior and inhibition of histaminergic neurons by LPS challenge

Infusion of the reversible anesthetic bupivacaine into the dorsal vagal complex directly prior to LPS treatment reversed the inhibitory effect of LPS on the exploratory behavior (DVC infusion × i.p. treatment interaction $F(1,13) = 7.48$, $p = 0.017$). Maze arm entries by rats, which received intra-DVC bupivacaine and i.p. LPS, were not significantly different in number from entries by those injected i.p. with saline (Fig. 5A). In contrast, rats infused with saline into the DVC and intraperitoneally challenged with LPS made significantly fewer arm entries and showed slowed locomotion and brief moments of immobility, similar to the unoperated LPS-treated rats tested in the EPM (described above).

In the brain, inactivation of the DVC diminished the inhibitory effect of LPS treatment on c-Fos expression in HDC-positive neurons of the VTM (Fig. 5B, 6). Exploration-associated c-Fos induction in the HDC-immunoreactive neurons of the VTM, expressed as the proportion of the total number of HDC-positive cell bodies counted, was significantly inhibited by LPS challenge in rats that were infused with vehicle into the DVC ($p < 0.05$). Following infusion of bupivacaine into the DVC, however, the difference between the LPS- and saline-injected groups in the proportion of HDC-positive cell bodies that showed nuclear immunostaining for c-Fos was much smaller and did not reach significance.

LPS-responsive afferents of the VTM

Of the 14 brains in which Fluorogold was administered, 9 cases showed FG deposits that encompassed the ventral tuberomammillary nucleus containing the E1-3 histaminergic neurons (depicted in Fig. 7A), whereas the other cases were omitted because the FG deposits were close to but largely outside the VTM. In addition to the VTM, FG spread into the ventral-most portions of the posterior lateral hypothalamus, the premammillary and lateral mammillary nuclei, but the area of deposit remained ventral to the fornix (see representative photomicrograph in Fig. 7B). The lateral perifornical and parasubthalamic regions of the hypothalamus remained outside the area of tracer spread. Retrogradely labeled neurons were identified by the fine granular cytoplasmic labeling in the neuronal cell bodies and proximal dendrites. Such neurons were present throughout the adjacent lateral and anterior, as well as medial preoptic portions of the hypothalamus, the intermediate lateral septum, and the infralimbic cortex, as described previously (Ericson et al., 1991), albeit in low numbers in the latter two regions. FG and c-Fos double-labeled neurons were rather sparse and, in the ventrolateral and medial preoptic regions, occurred in both LPS- and saline-treated animals. More caudally, FG-labeled neurons resided in the dorsal and ventral tegmental nuclei in the pons. Very few cells were present in the pericoerular region or the locus coeruleus itself in about half of the cases. In all cases, FG-labeled cells were distributed throughout the rostral, intermediate and caudal portions of the VLM, and also harbored the medial and the commissural parts of the NTS, extending most rostrally to where the NTS recedes from the fourth ventricle and caudally to where the NTS is enclosed dorsally by the gracile nucleus. Although the total number of labeled neurons in the brainstem varied per case, FG-labeled brainstem neurons were consistently more numerous in the VLM than in the NTS (approximately at a 80%–20% ratio). Nuclear c-Fos staining was vityually absent in FG-labeled cells in the medulla of saline-treated rats (Fig. 7C). LPS treatment, however, resulted in the induction of nuclear c-Fos immunoreactivity in many FG-labeled neurons encountered in the VLM and NTS (Fig. 7D), but not in other brain regions populated by FG-labeled cells.

Catecholaminergic phenotype of LPS-responsive medullary afferents—Triple labeling for c-Fos immunoreactivity and immunofluoresence labeling for FG (amplified with Alexa Fluor 488) and DBH (labeled with Alexa Fluor 546) showed many retrogradely labeled neurons with nuclear c-Fos staining (visible with complementary brightfield illumination) and concurrent DBH immunofluorescence in the NTS and the VLM (Fig. 8). Counts of labeled neurons and calculated proportions revealed that a large percentage of all retrogradely labeled neurons expressed nuclear c-Fos immunoreactivity following LPS treatment (NTS: 49%, VLM: 58%), but not after saline injection (NTS: 6%, VLM: 2%;Fig. 9A). The greater majority of FG-labeled neurons expressed the DBH-positive phenotype, (NTS: 69%, VLM: 84%; Fig. 9B). LPS challenge induced c-Fos staining in an even larger proportion of the DBH-FG double-labeled neurons (NTS: 60%, VLM: 69%; Fig. 9C). Among the FG and c-Fos double-labeled neurons (i.e., VTM-projecting neurons that were activated following LPS challenge), the greater majority in the NTS (77%), and virtually all of them in the VLM (99%) displayed additional DBH immunofluorescence (Fig. 9D). The distribution of the triple-labeled cell bodies included the portions of the VLM and medial NTS rostral to the obex, which harbor adrenergic (C1 and C2) neurons as well as the more caudally portions of the VLM and NTS that harbor noradrenergic (A1 and A2) cell groups. The contribution of the adrenergic population was not confirmed, however, as DBH immunoreactivity does not distinguish between the adrenergic and noradrenergic phenotypes. In and around the locus coerulus, present in very low numbers if any, the majority of the FG-labeled neurons were DBH-negative, and among the few FG-DBH-labeled cells encountered, none were c-Fos-positive irrespective of LPS or saline treatment.

Catecholaminergic innervation of the VTM—A dense plexus of DBH-immunoreactive fibers and varicosities was prevalent in the posterior basal hypothalamus with apparent preference for the tuberomammillary nucleus where numerous DBH-immunoreactive fibers and varicosities intermingled with the ADA-positive magnocellular neurons in all subdivisions of the VTM (Fig. 10A; ADA is another reliable marker for histaminergic neurons, see the methods section). In fact, the density of DBH-positive fibers is much lower in the adjacent portions of the posterior hypothalamus such as the lateral mammillary and the dorsal and ventral premammillary nuclei. Although in considerably lower density, PNMT-immunoreactive fibers and terminal boutons were present predominantly within the ADA-cell rich portions of the VTM (Fig. 10B), and were much sparser in the adjacent nuclei, a pattern similar to that described for the DBH-positive fibers. Close appositions of both DBH- (Fig. 10C) and PNMT-labeled varicosities (Fig. 10D) appeared with individual ADA-immunoreactive cell bodies and dendrites (indicated with arrows).

DISCUSSION

The present study shows that, with c-Fos expression as a marker, activation of histaminergic neurons in the VTM correlates consistently with behavioral arousal in exploration of a novel environment, social interaction and food intake, and that prior challenge with the pro-inflammatory stimulus LPS dramatically inhibited, if not prevented, this activation concomitant with reduced behavioral activity. These observations indicate that functional activation of the histaminergic system associated with behavioral arousal appears to be disrupted during peripheral inflammation associated sickness. In addition, the experiments in this study provide evidence that this disruption likely involves posterior hypothalamic input from LPS-responsive nuclei in the lower brainstem, because inactivation of the dorsal vagal complex reversed the suppressive effect of LPS on histaminergic neurons, and restored exploratory activity in a novel environment. Moreover, predominantly catecholaminergic neurons in the NTS and the VLM, many of them LPS-responsive, may provide the functional link between the caudal brainstem and the histaminergic system via direct projections to the VTM as demonstrated in this study, through which peripheral immune activation exerts a

functional inhibition of the histaminergic neurons. Taken together, these findings suggest that functional inhibition of the histaminergic system may constitute an important neuronal basis of behavioral symptoms during illness, i.e., reduced behavioral arousal and activity, and that catecholaminergic neurons of the caudal medulla contribute to the suppression of the activity of the histaminergic system (Fig. 11).

The histaminergic system and behavioral arousal

The different behavioral paradigms share in common that they all activate the ventral tuberomammillary nucleus and its histaminergic neurons as revealed with c-Fos immunostaining. The behavioral arousal experienced by the rats represents one common characteristic among all tests to allow them to engage in goal-directed behavior, and activation of histaminergic system may represent a critical neurobiological phenomenon that drives behavioral arousal and engagement, independent of specific types of behavior. This concept is also corroborated by previous studies that show a strong and consistent correlation of c-Fos induction in histaminergic neurons with an aroused waking state and behavioral activity, rather than sleep or quiet wakefulness (Ko et al., 2003). The induction of c-Fos protein in histaminergic neurons correlates highly with anticipatory and motivational behavioral activities in the context of restricted food availability and the expression of c-*fos* mRNA precedes activation of other arousal-supporting systems (Meynard et al., 2005; Valdes et al., 2005), which supports a mediating role for the histaminergic system in behavioral arousal. The induction of c-Fos in the VTM in the context of the behavioral experiments described in the present study appeared strong, with the greater majority of identified histaminergic neurons (up to 80%) showing expression of this activation marker in the EPM exploration test. It is unlikely that the histaminergic system represents a critical component of stress response to internal or external threat, as c-Fos induction in the VTM in different stress paradigms is limited (Miklos and Kovacs, 2003). The present results corroborate the limited response of the VTM to LPS injection itself in home cage controls as an example of a stress stimulus of visceral or internal origin. The lack of c-Fos immunoreactivity in histaminergic neurons of rats that were left undisturbed in their home cage coincides with very limited behavioral activity during the diurnal phase when rats spend most of their time resting or sleeping (as reported byKo et al., 2003), either when injected with LPS or saline. The present observations provide further support to the notion that the histaminergic system plays a pivotal role in alert waking states and motivated, goal-directed behaviors, but do not provide conclusive evidence that the activation of histaminergic neurons is necessary for behavioral arousal to occur, because of the correlational, rather than causational, character of the behavioral and neuronal activation data. However, in conjunction with previous studies that do allude to an indispensable role for the histaminergic system in behavioral performance (Parmentier et al., 2002), the current findings provide strong support for the idea that sickness behavior, at least in part, is mediated by functional inhibition of the histaminergic system in response to proinflammatory challenge.

The histaminergic system and sickness behavior

In each of the behavioral paradigms applied, LPS challenge virtually eliminated the c-Fos induction in the histaminergic neurons in the VTM normally seen in saline-treated rats in response to behavioral challenge. Such inhibition or disruption of functional engagement of the histaminergic system reveals a potentially important mechanism underlying the typical behavioral symptoms of sickness, including psychomotor slowing, experience of fatigue, apathy, impaired vigilance, and sleepiness, of which neural mechanisms and pathways have remained elusive thus far (Dantzer, 2001). Because the bulk of previous studies of brain responses to inflammatory challenges using c-Fos as a marker involved animals that remained in their home cage and during their inactive phase, inhibitory events among components of the neurocircuitry underlying sickness behavior remained unnoticed. Inhibitory events initiated by pro-inflammatory insult would become apparent, however, when an active behavioral context

is chosen as the reference condition as applied in this study, revealing a seemingly disengaged histaminergic system in LPS-treated rats despite the stimulatory behavioral context of a novel environment, social cues, or highly palatable food. Deficient histaminergic neurotransmission, as seen in L-HDC-/- transgenic mice, is associated with perturbed sleep and cortical EEG patterns and reduced behavioral responsiveness to a novel environment (Parmentier et al., 2002), thus showing some resemblance to the behavioral changes observed in LPS-treated rats. The activation of the histaminergic system, critical for adequate behavioral responses, and the apparent lack thereof in LPS-treated rats, supports our hypothesis that an inhibitory drive on the histaminergic system contributes to behavioral symptoms of sickness.

Mechanisms of LPS-induced inhibition of histaminergic neurons

This study provides evidence that lower brainstem afferents may be implicated in functional inhibition of the VTM histaminergic system. Inactivation of the dorsal vagal complex reduced the suppressive effect of LPS on exploratory behavior and restored activation of the histaminergic system, and a significant proportion of neurons in the VLM and the NTS that were retrogradely labeled with Fluorogold from the ventral tuberomammillary region are responsive to LPS challenge. Most of these LPS-responsive FG-labeled neurons express DBH, which is expressed in the C1/C2 adrenergic and A1/A2 noradrenergic neurons in the VLM and the NTS. Our current findings are consistent with the consensus that caudal medullary afferents originating in the VLM and NTS provide the major bulk of noradrenergic and adrenergic innervation to the tuberomammillary nucleus in the ventral posterior hypothalamus (Ericson et al. 1989, this study), as well as to the various other components of the hypothalamus, including the paraventricular nucleus (Sawchenko and Swanson, 1982) and the lateral hypothalamus (Palkovits et al., 1992). It is possible that the LPS-responsive ascending catecholaminergic projections give rise to collaterals to the various hypothalamic targets enabling activation of the paraventricular nucleus and suppression the histaminergic system in a coordinated fashion in response to an inflammatory insult.

Because the FG injection sites extended beyond the limits of the VTM proper, we cannot preclude the possibility that the retrograde labeling of DBH-positive neurons in the VLM and NTS derives from fibers innervate more dorsal areas of the ventral hypothalamus rather than the histaminergic cell-rich VTM. However, the plexus of DBH- and PNMT-immunoreactive fibers is densest in the histamine cell-rich portion of the VTM and rather sparse in the immediate vicinity (Fig. 10). Since PNMT-labeled fibers in the hypothalamus derive exclusively from caudal medullary sources (Palkovits et al., 1992), and the predominant source of DBH-labeled innervation in the hypothalamus derives from the caudal medulla (Sawchenko and Swanson, 1982), it can be inferred at least that retrogradely labeled DBH-positive neurons in the NTS and VLM indeed provide input to the VTM that are functionally relevant in the context of LPS challenge, as many of these were triple-labeled for FG, DBH and c-Fos. With reference to the occurrence of triple-labeled neurons, the contribution from the locus coeruleus, another possible source of noradrenergic input, was notably absent. Based on our further observations that many DBH- and PNMT-labeled varicosities abut the histaminergic cell bodies and dendrites (Fig. 10), it can be concluded with reasonable confidence that there is a rather direct influence on the histaminergic neurons exerted by the catecholaminergic neurons of the NTS and VLM, many of which become functionally activated by LPS challenge.

The majority of the retrogradely labeled LPS-responsive afferents (i.e, neurons double-labeled for FG- and c-Fos) in the caudal medulla were located in the VLM. This finding may at first seem inconsistent with the finding that inactivation of the DVC prevented suppression of c-Fos induction in the VTM following LPS treatment. However, the NTS and VLM give rise to dense reciprocal connections and are functionally linked (Sawchenko and Swanson, 1982; Ross et al., 1985; Kawano et al., 1996; Yu and Gordon, 1996). In particular, the adrenergic C1

and noradrenergic A1 neurons in the VLM receive significant input from the NTS (Aicher et al., 1996; Chan et al., 1995). In turn, during LPS challenge, VLM projection fibers provide the majority of immune-responsive input to the paraventricular hypothalamus (PVN; Gaykema et al. 2007; Buller et al. 2001). Although catecholaminergic projection neurons from both the NTS and VLM respond to viscerosensory information, those associated with the VLM seem to respond selectively to more serious homeostatic challenge, including glucoprivation (Ritter et al. 2001), hypovolemia (Potts et al. 2000), and immune challenge (Ericsson et al. 1994, Ericsson et al. 1994; Gaykema et al. 2007; Goehler et al., 2005). Thus the catecholaminergic neurons in the VLM, more than those in the NTS may contribute to neurocircuitry that specifically responds to challenge or "danger" of viscerosensory origin.

Although these findings support the idea that ascending and predominantly catecholaminergic projections from the lower brainstem to the hypothalamus exert inhibitory effect on the VTM histaminergic neurons in the context of LPS challenge, the possibility that these projections exert direct inhibitory control of histaminergic neurons of the VTM, however, needs further examination. Contrary to this notion, a recent electrophysiological study using brain slices demonstrated α_2 adrenergic receptor-mediated inhibition of GABAergic inhibitory postsynaptic potentials in putative histaminergic neurons resulting in their disinhibition (Stevens et al., 2004). This finding would predict the noradrenergic input to be arousal-promoting, but such role would need to be confirmed *in vivo* when extrinsic input is intact. Indeed, ascending drive from the caudal medulla appears to exert arousing or sedating actions depending upon the context. For example, "satiety" signals (e.g., cholecystokinin) known to activate hypothalamic noradrenergic input from the lower brainstem (Rinaman et al., 1995) do have a mildly sedating effect, whereas medullary catecholaminergic input of the hypothalamus related to hypercapnia may contribute to behavioral arousal (Haxhiu et al., 2001; Johnson et al., 2005), and those responsive to glucoprivic conditions induced by insulin or 2-deoxy glucose injections would generate feeding responses (Ritter et al., 2001). Thus, LPS challenge may activate a subtly different population of medullary catecholaminergic neurons than those associated with arousing stimuli such as hypercapnia or glucoprivation but may overlap with those driven by, e.g., satiety factors associated with sedation.

Although our findings suggest that the medullary catecholaminergic projections may mediate the functional inhibition of the histaminergic system as a result of the LPS challenge, it remains to be established whether the functional inhibition of the histaminergic system occurs via direct and local interaction with catecholaminergic input, or indirectly via other distant sources of input. In the nearby lateral and perifornical hypothalamus, neurons containing orexin A and B (also referred to as hypocretin-1 and 2) provide a powerful excitatory drive on histaminergic neurons (Yamanaka et al., 2002), and are generally inhibited by noradrenaline and adrenaline (Yamanaka et al., 2006) provided by projections from the caudal medulla. Indeed, LPS has been reported to inhibit c-Fos induction feeding-related neurons in the lateral hypothalamus (Gautron et al. 2005), including orexin neurons (Becskei et al. 2007). Thus, these orexin neurons could constitute an additional, indirect link by which brainstem ascending pathways modulate the activity of histaminergic neurons by imposing an inhibitory influence on orexin neurons that normally activate histaminergic neurons (Yamanaka et al., 2002). Both the orexin and histaminergic system represent critical hypothalamic elements of the arousal-supporting neurocircuitry (Saper et al., 2005). Other sources of input that may contribute to LPS-induced inhibition of the histaminergic neurons include a group of GABAergic galanin-containing neurons in the ventrolateral preoptic area, which provide a major inhibitory input to the histaminergic system and which serve a sleep-promoting role (Sherin et al., 1996; 1998), but effects of pro-inflammatory challenge on these particular VLPO neurons is currently lacking. Further studies are clearly needed to elucidate the complex modulatory influence of ascending catecholaminergic pathways on the histaminergic neurons.

CONCLUSION

In conclusion, the present findings provide evidence for a prominent role for the histaminergic system in illness-associated behavioral depression. Behavioral arousal and engagement in goal-directed behavioral activity consistently correlates with a strong activation of histaminergic neurons, which is disrupted by peripheral pro-inflammatory challenge with LPS. This inhibitory influence on the central histaminergic system may constitute one of the mechanisms that underlie diminished behavioral activity and apparent state of hypo-arousal seen in LPS-treated rats displaying sickness symptoms. The inflammation-driven inhibitory drive on the histaminergic system appears to originate in the DVC, and catecholaminergic neurons in the caudal medulla serve a potential source for this inhibitory influence. The ascending catecholaminergic projections, both directly from the NTS and indirectly from the DVC through the VLM, to the VTM may constitute a component of the still poorly understood neurocircuitry that mediates sickness-associated behavioral symptoms, not only in acute but also in chronic conditions. This novel mechanism (depicted in Fig. 11) may provide an avenue for intervening treatments for the neurobehavioral symptoms that are associated with chronic inflammatory disease, cancer, and immunotherapy, and which share common characteristics with major depression (Capuron et al., 2002; (Raison and Miller, 2003).

Acknowledgements

References

Aiche SA, Saravay RH, Cravo S, Jeske I, Morrison SF, Reis DJ, Milner TA. Monosynaptic projections from the nucleus tractus solitarii to C1 adrenergic neurons in the rostral ventrolateral medulla: comparison with input from the caudal ventrolateral medulla. J Com Neurol 1996;373:62–75.

Becskei C, Riediger T, Hernadfalvy N, Arsenijevic D, Lutz TA, Langhans W. Inhibitory effects of lipopolysaccharide on hypothalamic nuclei implicated in the control of food intake. Brain Behav Immun. 2007epub ahead of print

Buller K, Xu Y, Dayas C, Day T. Dorsal and ventral medullary catecholamine cell groups contribute differentially to systemic interleukin-1β-induced hypothalamic pituitary adrenal axis responses. Neuroendocrinol 2001;73:129–138.

Buller KM, Day TA. Systemic administration of interleukin-1β activates select populations of central amygdala afferents. J Comp Neurol 2002;452:288–296. [PubMed: 12353224]

Burgdorf J, Panksepp J. Tickling induces reward in adolescent rats. Physiol Behav 2001;72:167–173. [PubMed: 11239994]

Capuron L, Gumnick JF, Musselman DL, Lawson DH, Reemsnyder A, Nemeroff CB, Miller AH. Neurobehavioral effects of interferon-α in cancer patients: phenomenology and paroxetine responsiveness of symptom dimensions. Neuropsychopharmacol 2002;26:643–652.

Chan RKW, Peto C, Sawchenko PE. A1 catecholaminergic cell group: fine structure and synaptic input from the nucleus of the solitary tract. J Comp Neurol 1995;351:62–80. [PubMed: 7896940]

Dantzer R. Cytokine-induced sickness behavior: where do we stand? Brain Behav Immun 2001;15:7–24. [PubMed: 11259077]

Elmquist JK, Scammell TE, Jacobson CD, Saper CB. Distribution of Fos-like immunoreactivity in the rat brain following intravenous lipopolysaccharide administration. J Comp Neurol 1996;371:85–103. [PubMed: 8835720]

Ericson H, Watanabe T, Kohler C. Morphological analysis of the tuberomammillary nucleus in the rat brain: delineation of subgroups with antibody against L-histidine decarboxylase as a marker. J Comp Neurol 1987;263:1–24. [PubMed: 2822770]

Ericson H, Blomqvist A, Kohler C. Brainstem afferents to the tuberomammillary nucleus in the rat brain with special reference to monoaminergic innervation. J Comp Neurol 1989;281:169–192. [PubMed: 2565348]

Ericson H, Blomqvist A, Kohler C. Origin of neuronal inputs to the region of the tuberomammillary nucleus of the rat brain. J Comp Neurol 1991;311:45–64. [PubMed: 1719044]

Ericsson A, Kovacs KJ, Sawchenko PE. A functional anatomical analysis of central pathways subserving the effects of interleukin-1 on stress-related neuroendocrine neurons. J Neurosci 1994;14:897–913. [PubMed: 8301368]

Ericsson A, Arias C, Sawchenko PE. Evidence for an intramedullary prostaglandin-dependent mechanism in the activation of stress-related neuorendocrine circuitry by intravenous interleukin-1. J Neurosci 1997;17:7166–7179. [PubMed: 9278551]

Gautron I, Mingam R, Moranis A, Combe C, Laye S. Influence of feeding status on neuronal activity in the hypothalamus during lipopolysaccharide-induced anorexia in rats. Neurosci 2005;134:933–946.

Gaykema RPA, Chen C-C, Goehler LE. Organization of immune-responsive medullary projections to the bed nucleus of the stria terminalis, central amygdala, and paraventricular nucleus of the hypothalamus: evidence for parallel viscerosensory pathways in the rat brain. Brain Res 2007;1130:130–145. [PubMed: 17169348]

Goehler LE, Gaykema RPA, Opitz N, Reddaway R, Badr NA, Lyte M. Activation in vagal afferents and central autonomic pathways: early responses to intestinal infection with *Campylobacter jejuni*. Brain Behav Immun 2005;19:334–344. [PubMed: 15944073]

Haas H, Panula P. The role of histamine and the tuberomammillary nucleus in the nervous system. Nature Rev Neurosci 2003;4:121–130. [PubMed: 12563283]

Hart BL. Biological basis of the behavior of sick animals. Neurosci Biobehav Rev 1988;12:123–137. [PubMed: 3050629]

Haxhiu MA, Tolentino-Silva F, Pete G, Kc P, Mack SO. Monoaminergic neurons, chemosensation and arousal. Respiration Physiol 2001;129:191–209.

Huang ZL, Qu WM, Li WD, Mochizuki T, Eguchi N, Watanabe T, Urade Y, Hayaishi O. Arousl effect of orexin A depends on activation of the histaminergic system. Proc Natl Acad Sci USA 2001;98:9965–9970. [PubMed: 11493714]

Inoue I, Yanai K, Kitamura D, Taiuchi I, Kobavachi T, Niimura KK, Watanabe T, Watanabe T. Impaired locomotor activity and exploratory behavior in mice lacking H1 receptors. Proc Natl Acad Sci USA 1996;93:13316–13320. [PubMed: 8917588]

Johnson PL, Moratalla R, Lightman SL, Lowry CA. Are tuberomammillary histaminergic neurons involved in CO_2-mediated arousal? Exp Neurol 2005;193:228–233. [PubMed: 15817281]

Kawano H, Masuko S. Neurons in the caudal ventrolateral medulla projecting to the paraventricular hypothalamic nucleus receive synaptic inputs from the nucleus of the solitary tract: a light and electron microscopic double-labeling study in the rat. Neurosci. Lett 1996;218:33–36. [PubMed: 8939474]

Ko EM, Estabrooke IV, McCarthy M, Scammell TE. Wake-related activity of tuberomammillary neurons in rats. Brain Res 2003;992:220–226. [PubMed: 14625060]

Konsman JP, Kelley K, Dantzer R. Temporal and spatial relationships between lipopolysaccharide-induced expression of Fos, interleukin-1β and inducible nitric oxide synthase in rat brain. Neurosci 1999;89:535–548.

Lin JS, Sakai K, Vanni-Mercier G, Jouvet M. A critical role of the posterior hypothalamus in the mechanisms of wakefulness determined by microinjection of muscimol in freely moving cats. Brain Res 1989;479:225–240. [PubMed: 2924157]

Lin JS. Brain structures and mechanisms involved in the control of cortical activation and wakefulness, with emphasis on the posterior hypothalamus and histaminergic neurons. Sleep Med Rev 2000;4:471–503. [PubMed: 17210278]

Marvel FA, Chen C-C, Badr NA, Gaykema RPA, Goehler LE. Reversible inactivation of the dorsal vagal complex blocks lipopolysaccharide-induced social withdrawal and c-Fos expression in central autonomic nuclei. Brain Behav Immun 2004;18:123–143. [PubMed: 14759590]

Meynard MM, Valdes JL, Recabarren M, Seron-Ferre M, Torrealba F. Specific activation of histaminergic neurons during daily feeding anticipatory behavior in rats. Behav Brain Res 2005;158:311–319. [PubMed: 15698898]

Miklos IH, Kovacs KJ. Functional heterogeneity of the responses of histaminergic neuron subpopulations to various stress challenges. Eur J Neurosci 2003;18:3069–3079. [PubMed: 14656302]

Palkovits M, Mezey E, Skirboll LR, Hokfelt T. Adrenergic projections for the lower brainstem to the hypothalamic paraventricular nucleus, the lateral hypothalamic area and the central nucleus of the amygdala in rats. J Chem Neuroanat 1992;5:407–415. [PubMed: 1418754]

Parmentier R, Ohtsu H, Djebbara-Hannas Z, Valatx J-L, Watanabe T, Lin J-S. Anatomical, physiological, and pharmacological characteristics of histidine decarboxylase knock-out mice: evidence for the role of brain histamine in behavioral and sleep-wake control. J Neurosci 2002;22:7695–7711. [PubMed: 12196593]

Paxinos, G.; Watson. The Rat Brain in Stereotaxic Coordinates. Fourth Ed.. San Diego, CA: Academic Press; 1998.

Potts PD, Ludbrook J, Gillman-Gasapri TA, Horiuchi J, Dampney RAL. Activation of brain neurons following central hypervolemia and hypovolemia: contributions of baroreceptive and non-baroreceptive inputs. Neurosci 2000;95:499–511.

Raison CL, Miller AH. Depression in cancer: new developments regarding diagnosis and treatment. Biol Psychiatry 2003;54:283–294. [PubMed: 12893104]

Rinaman L, Hoffman GE, Dohanics J, Le WW, Stricker EM, Verbalis JG. Cholecystokinin activates catecholaminergic neurons in the caudal medulla that innervate the paraventricular nucleus of the hypothalamus in rats. Comp Neurol 1995;360:246–258.

Ritter S, Bugarith K, Dinh TT. Immunotoxic destruction of distinct catecholamine subgroups produces selective impairment of glucoregulatory responses and neuronal activation. J Comp Neurol 2001;432:197–216. [PubMed: 11241386]

Ross CA, Ruggiero DA, Reis DJ. Projections from the nucleus tractus solitarii to the rostral ventrolateral medulla. J Comp Neurol 1985;242:511–534. [PubMed: 2418079]

Saper CB, Scammel TE, Lu J. Hypothalamic regulation of sleep and circadian rhythms. Nat 2005;437:1257–1263.

Sawchenko PE, Swanson LW. The organization of noradrenergic pathways from the brainstem to the paraventricular and supraoptic nuclei in the rat. Brain Res Rev 1982;4:275–375.

Senba E, Daddona PE, Watanabe T, Wu JY, Nagi JI. Coexistence of adenosine deaminase, histidine decarboxylase, and glutamate decarboxylase in hypothalamic neurons of the rat. J Neurosci 1985;5:3393–3402. [PubMed: 4078633]

Sherin JE, Elmquist JK, Torrealba F, Saper CB. Innervation of histaminergic tuberomammillary neurons by GABAergic and galaninergic neurons in the ventrolateral preoptic nucleus of the rat. J Neuosci 1998;18:4705–4721.

Sherin JE, Shiromani PJ, McCarley RW, Saper CB. Activation of ventrolateral preoptic neurons during sleep. Science 1996;271:216–218. [PubMed: 8539624]

Stevens DR, Kuramasu A, Eriksson KS, Selbach O, Haas HL. α2-adrenergic receptor-mediated presynaptic inhibition of GABAergic IPSPs in rat histaminergic neurons. Neuropharmacol 2004;46:1018–1022.

Takahashi K, Lin J-S, Sakai K. Neuronal activity of histaminergic tuberomammillary neurons during wake-sleep states in the mouse. J Neurosci 2006;26:10292–10298. [PubMed: 17021184]

Valdes JL, Farias P, Ocampo-Garces A, Cortes N, Seron-Ferre M, Torrealba F. Arousal and differential Fos expression in histaminergic neurons of the ascending arousal system during a feeding-related motivated behaviour. Eur J Neurosci 2005;21:1931–1942. [PubMed: 15869486]

Yamanaka A, Tsujino N, Funahashi H, Honda K, Guan J-I, Wang Q-P, Tominaga M, Goto K, Shiioda S, Sakurai T. Orexins activate histaminergic neurons via the orexin 2 receptor. Biochem Biophys Res Comm 2002;290:1237–1245. [PubMed: 11811995]

Yamanaka A, Muraki Y, Ichiki K, Tsujino N, Kilduff TS, Goto K, Sakurai T. Orexin neurons are directly and indirectly regulated by catecholamines in a complex manner. J Neurophysiol 2006;96:284–298. [PubMed: 16611835]

Yu D, Gordon FJ. Anatomical evidence for a bi-neuronal pathway connecting the nucleus tractus solitarius to caudal ventrolateral medulla to rostral ventrolateral medulla in the rat. Neurosci Lett 1996;205:21–24. [PubMed: 8867011]

Yoshida Y, Matsumura H, Nakajima T, Mandai M, Urakami T, Kuroda K, Yoneda H. Prostaglandin E (EP) receptor subtypes and sleep: promotion by EP_4 and inhibition by EP_1/EP_2. NeuroReport 2000;11:2127–2131. [PubMed: 10923657]

Abbreviations

ADA, adenosine deaminase
ANOVA, analysis of variance
DAB, diaminobenzidine
DBH, dopamine beta-hydroxylase
DVC, dorsal vagal complex
EPM, elevated plus maze
FG, Fluorogold
HDC, histidine decarboxylase
LPS, lipopolysaccharide
NTS, nucleus of the solitary tract
PNMT, phenylethanolamine-N-methyltransferase
VLM, ventrolateral medulla
VTM, ventral tuberomammillary nucleus
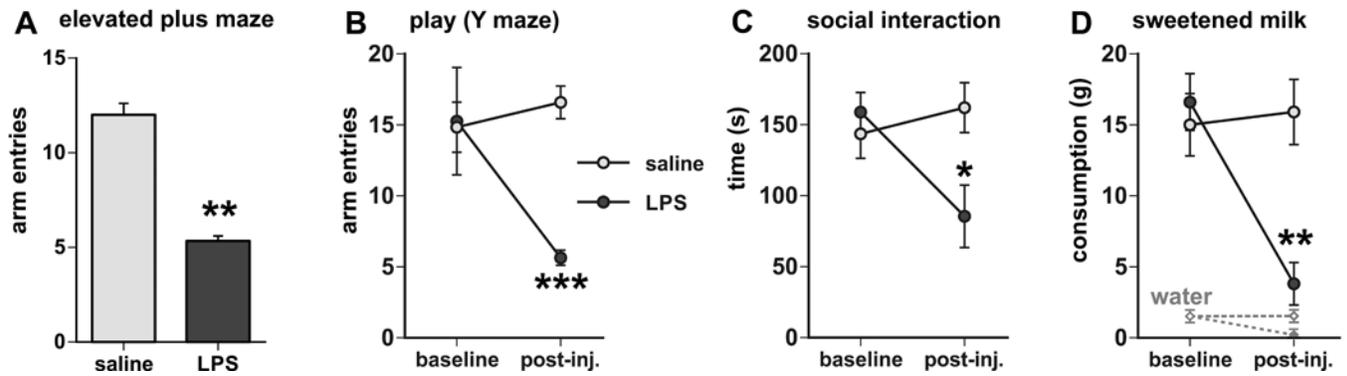
Fig. 1.
Behavioral activity is suppressed by prior treatment with LPS in the elevated plus maze-novel
environment exploration task, shown by the reduced number of arm entries (A). Similarly, LPS
treatment suppressed behavioral activity during playful activity in the Y maze (reduced number
of arm entries in B), during social interaction with a conspecific juvenile (reduced interaction
time in C), and during the presentation of sweetened milk (reduced consumption in D). The
graphs in B-D display the baseline values of the behavioral measures (averaged over the two
days prior to the day of experiment) in addition to the values following the injections of saline
or LPS (post-inj.). * $p < 0.05$, ** $p < 0.005$, *** $p < 0.0005$, LPS *vs.* saline treatment.
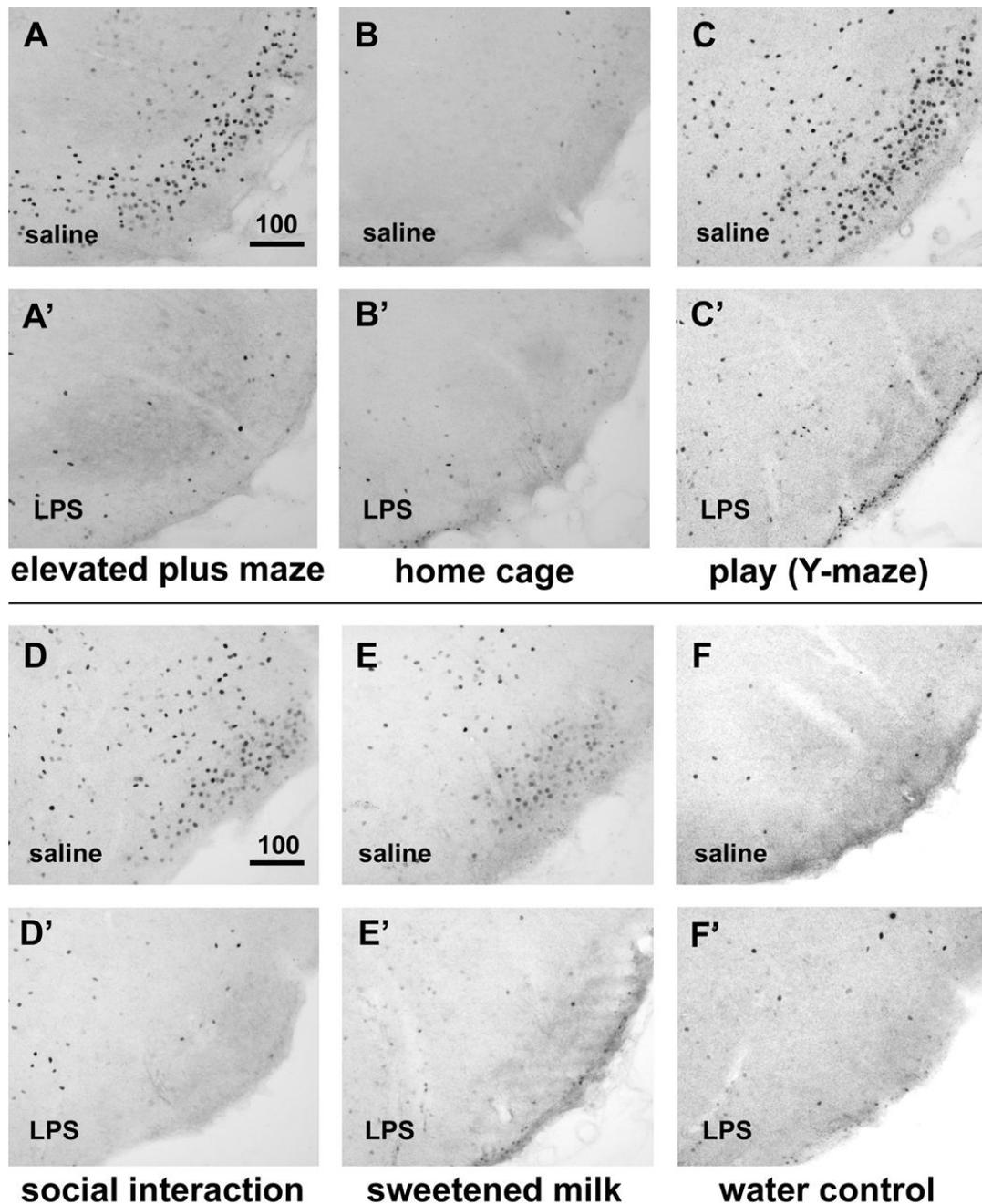
Fig. 2.
Induction of c-Fos immunoreactivity in the VTM associated with behavioral activation and
LPS-induced suppression. In saline-treated subjects, both exploration of a novel environment
(elevated plus maze, in A) and playful behavior (Y-maze, in C) induced strong neuronal c-Fos
expression that was absent in control animals left in the home cage (B). Behavioral activity in
the home cage such as social interaction (D) and consumption of sweetened milk (E) also lead
to induction, albeit more modest, of c-Fos immunoreactivity in the VTM, which was absent in
rats offered water instead (F). After LPS treatment, little c-Fos induction could be discerned
in the VTM irrespective of the behavioral context the animals were exposed to (EPM: A'; play/
Y-maze: C'; social interaction: D'; sweetened milk: E'), and the staining could not be

distinguished from that of LPS-treated rats left undisturbed in the home cage (B') or those offered water (F'). Scale bar in micrometers.
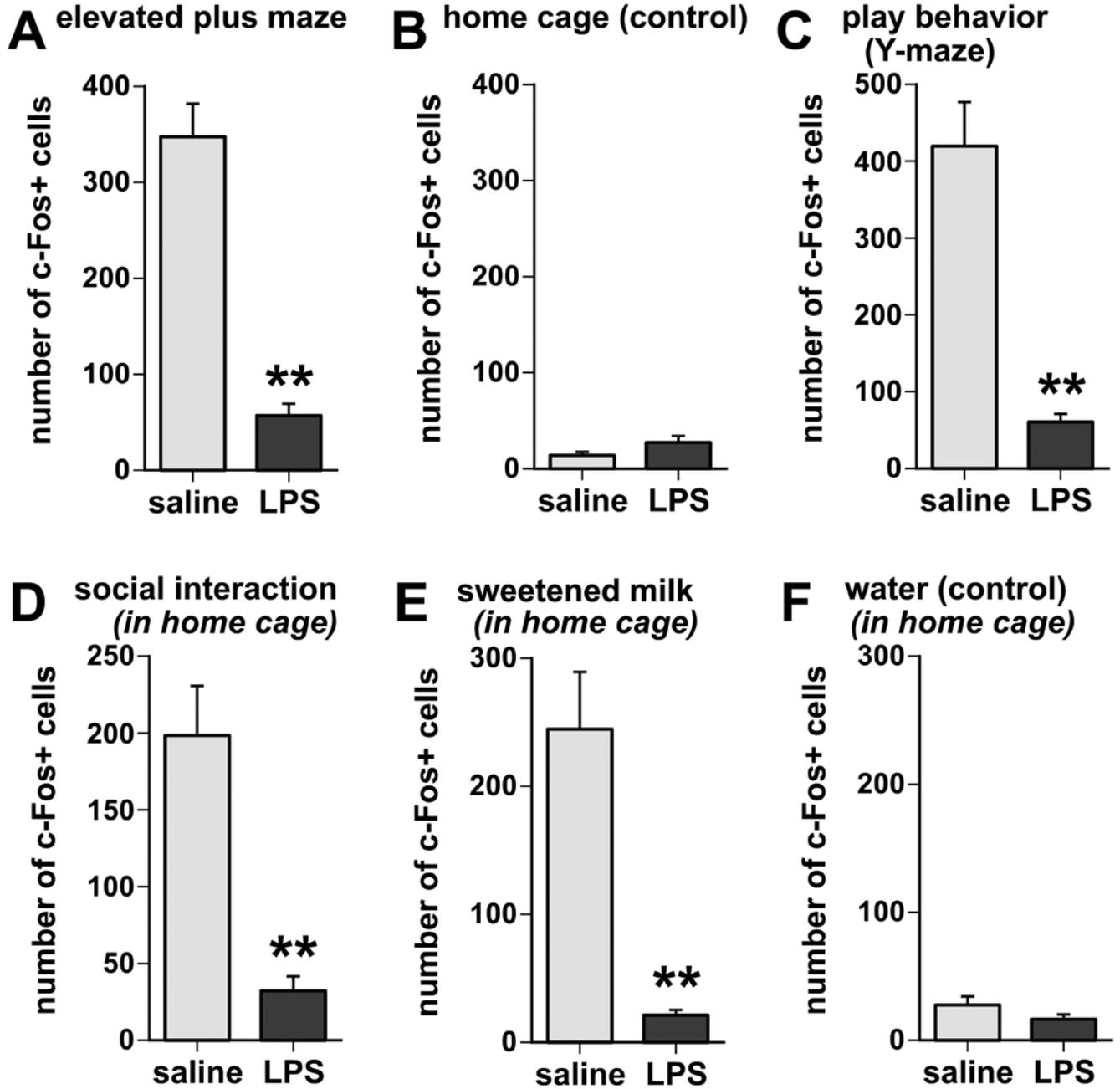
Fig. 3.
Semi-quantitative analysis of c-Fos-positive nuclei in the VTM reveals that LPS treatment strongly inhibited the induction of c-Fos immunoreactivity associated with exploratory (A), play behavior (B), social interaction (D), and sweetened milk consumption (D), whereas there was little c-Fos induction, and little or no difference between LPS and saline treatments, in home cage controls (B) or when offered water instead of sweetened milk (F). Values expressed represent means and SEM of cumulative counts in 4 sections through the posterior hypothalamus containing the E1-E3 regions of the VTM. ** $p < 0.005$, LPS *vs.* saline treatment.
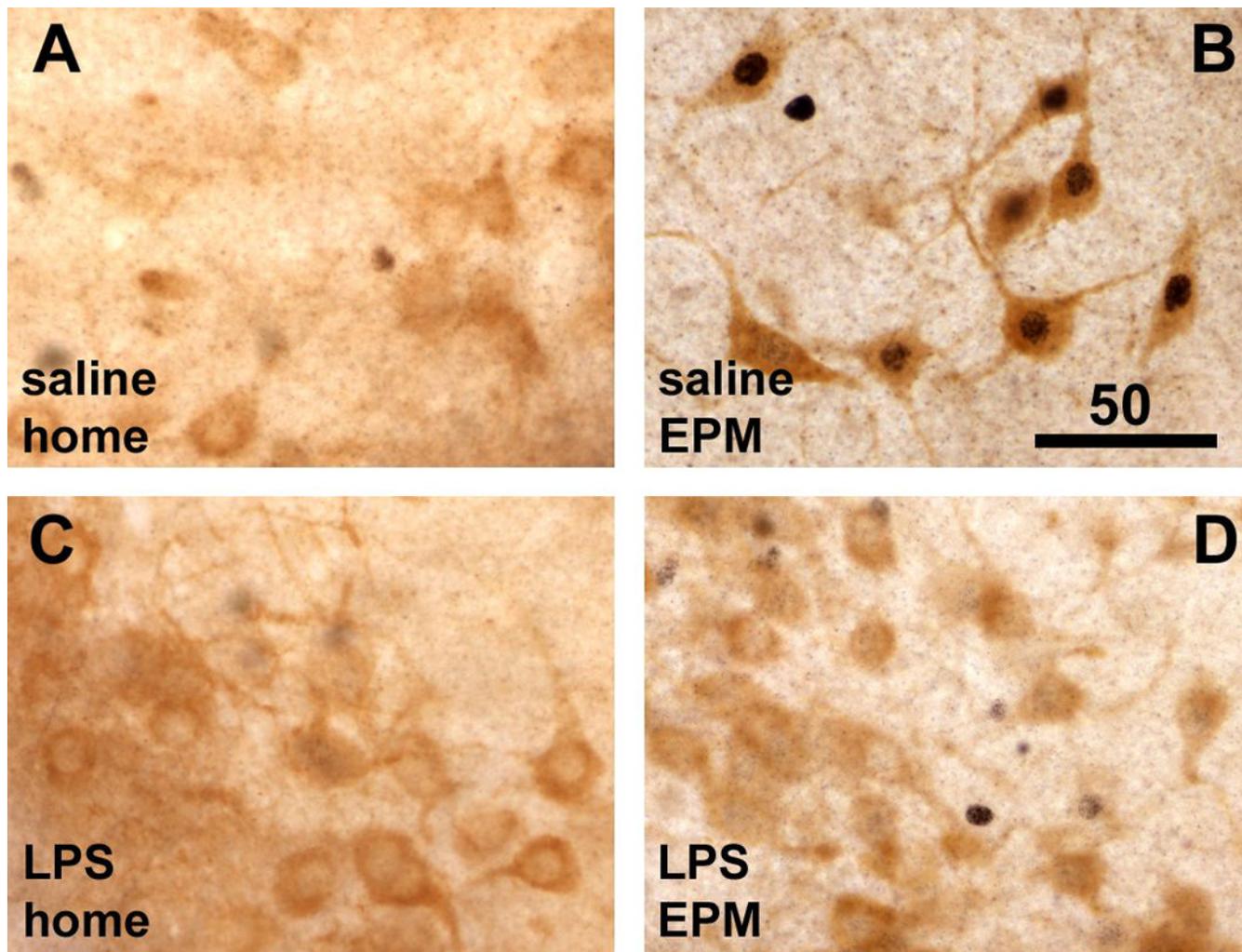
Fig. 4.
Double labeling for cytoplasmic L-histidine decarboxylase (HDC) and nuclear c-Fos immunoreactivity shows that HDC-positive neurons lacked nuclear c-Fos staining in home cage animals (A), but displayed strong nuclear staining for c-Fos (black) in rats 1 hour following EPM exploration (B). LPS challenge itself had little effect on c-Fos expression in HDC-positive neurons in home cage controls (C), but prior to the EPM test LPS challenge almost completely inhibited nuclear staining for c-Fos in HDC-positive neurons despite behavioral activity exhibited by the LPS-treated rats (D). Scale bar in B in µm. E. Semi-quantitative assessment of c-Fos immunoreactivity in HDC-positive (histaminergic) neurons revealed a strong induction in rats subjected to the exploration task, which was reversed by LPS challenge 90 minutes prior to the test (***, $p < 0.0001$). F. There was no difference between groups in the total number of HDC-positive cell bodies with visible cell nuclei (either c-Fos-labeled or unlabeled).
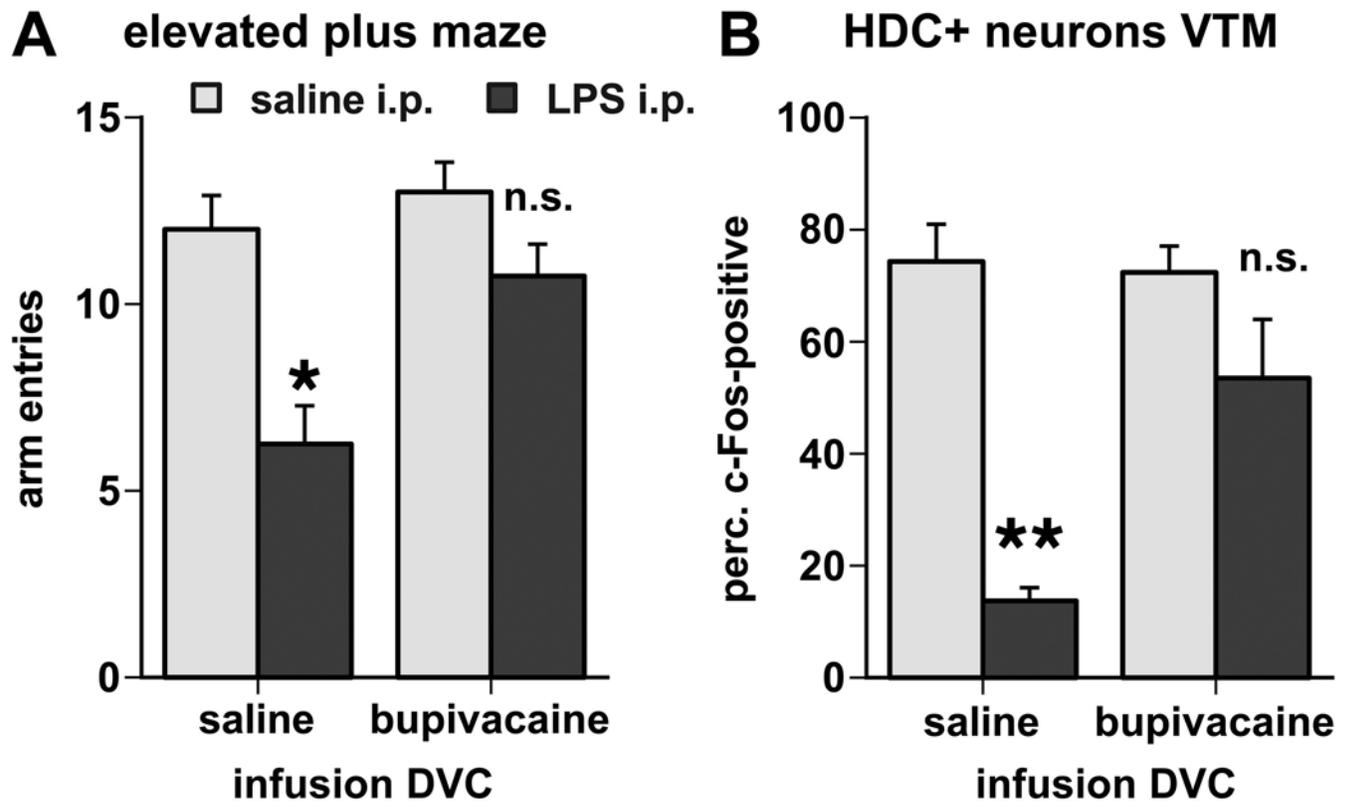
Fig. 5.
A. Inactivation of the dorsal vagal complex reversed the inhibitory effects of LPS challenge on behavioral activity during exploration of the elevated plus maze, as measured by the total number of arm entries. B. Inactivation of the DVC also diminished the suppressive effect of LPS on the c-Fos induction in histaminergic neurons associated with the exploratory behavior (LPS effects: *, $p < 0.01$; **, $p < 0.001$; n.s., not significant).
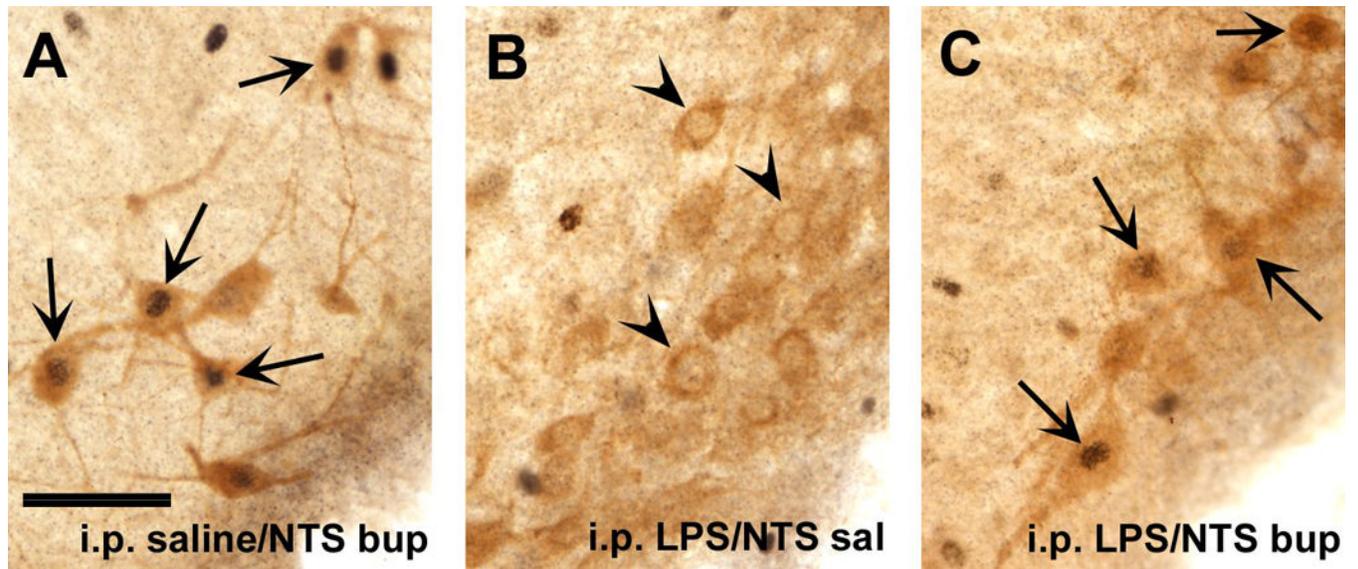
Fig. 6.
A. Induction of c-Fos immunoreactivity (black nuclear staining) in HDC-immunoreactive neurons in the VTM (lighter brown cytoplasmic staining) of a saline-treated rat following exploration of the elevated plus maze. Arrows point at double-labeled neurons. B,C. Following i.p. LPS challenge and maze exposure, c-Fos staining was absent in most HDC-labeled neurons, when saline was infused into the DVC (arrowheads in B), but appeared in HDC-positive neurons in LPS-treated rat that received intra-DVC bupivacaine infusion (arrows in C).
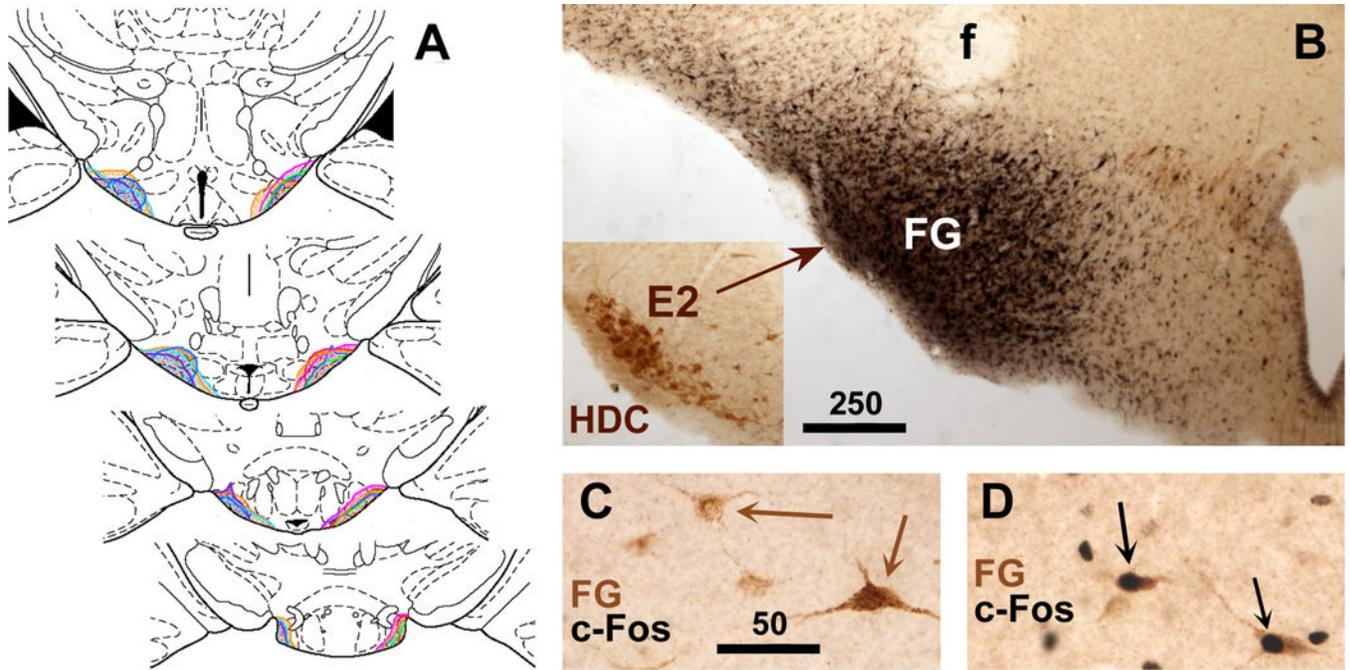
Fig. 7.
A. The extent of FG injection sites in the VTM shown in brain section diagrams (Paxinos and Watson, 1998) at 4 rostrocaudal levels through the posterior hypothalamus. FG injections of individual cases are indicated by color, and assembled together to show the rostrocaudal extent in each case. B. Photomicrograph of a representative FG injection site aimed at the VTM. FG immunoreactivity was visualized with black staining using nickelous DAB, whereas HDC immunoreactivity was revealed using regular DAB, yielding brown staining. The inserted photomicrograph shows HDC-containing neurons in the same location, taken from the opposite hemisphere in the same section, and presented after being flipped 180 degrees. C,D: In the NTS, retrogradely labeled neurons (displaying FG immunoreactivity stained brown using DAB) show black c-Fos immunostaining only after intraperitoneal LPS challenge (black arrows in D), but not after saline injection (brown arrows in C). Scale bars in B,C in micrometers.
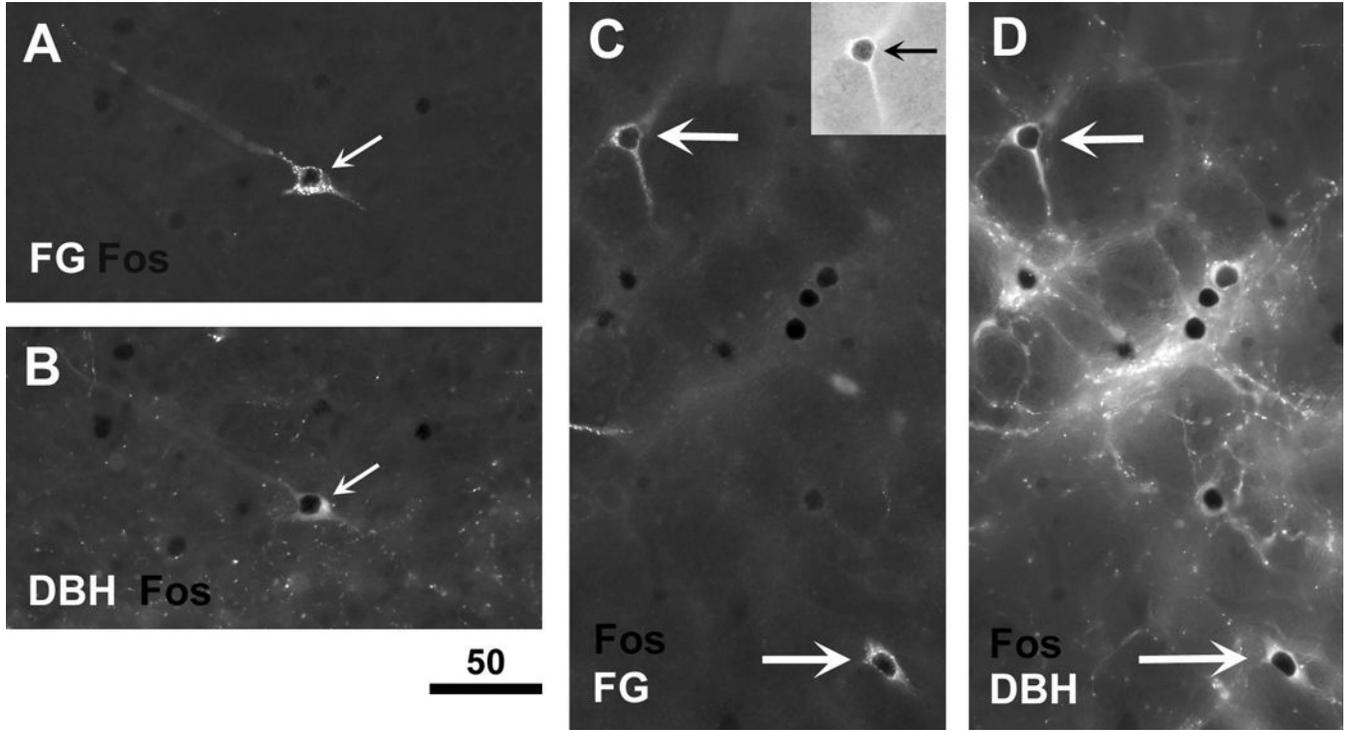
Fig. 8.
FG-positive neurons (retrogradely labeled from the VTM region) in the NTS (A,B) and VLM (C,D) that display LPS-induced c-Fos expression are predominantly DBH-positive. The triple staining was achieved by sequential immunofluoresence labeling for FG (Alexa Fluor 488 excitation, shown in A,C) and DBH (Alexa Fluor 546 excitation, shown in B,D), followed by initial immunoperoxidase staining for c-Fos as revealed by the intense black shadow (arrows) or staining visualized by complementary brightfield illumination (insert in the top right corner of panel C). The micrographs in A and B, and those in C and D, captured the same location in the NTS and VLM, respectively. Scale bar in micrometers.
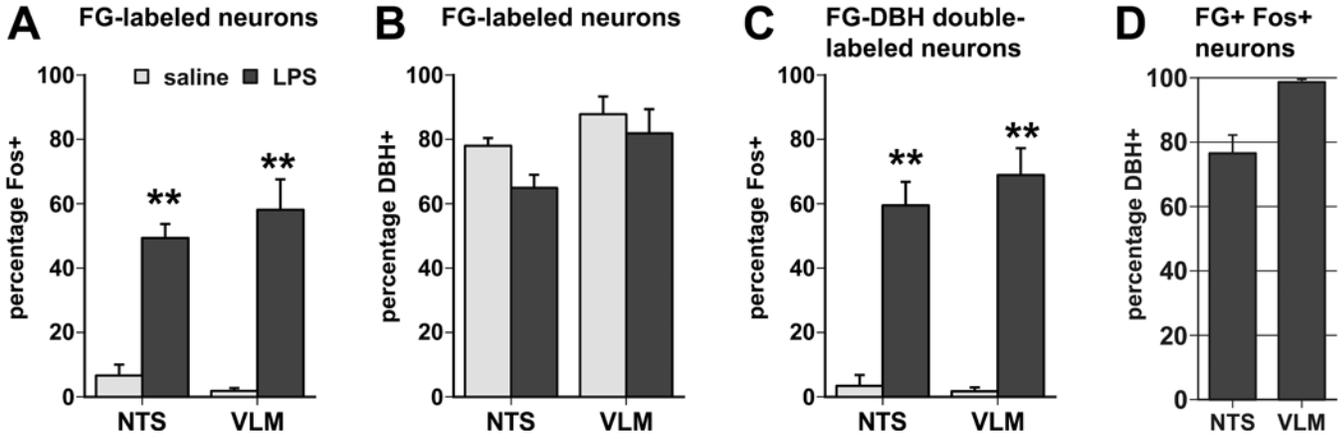
Fig. 9.
A. Semi-quantitative analysis of the induction of c-Fos expression by LPS challenge (0.1 mg/kg i.p.), but not saline injection, in FG-labeled neurons in the NTS and VLM (retrogradely labeled from the VTM region of the posterior hypothalamus). Values are expressed as the fraction of the total of retrogradely labeled neurons with a prominently visible nucleus in the plane of the section (**, $p < 0.005$). B. The FG-labeled neurons in the NTS and VLM predominantly show a noradrenergic/adrenergic phenotype as most display DBH immunoreactivity. C. LPS-mediated induction of c-Fos expression occurs in 60–70% of all FG-DBH-double-labeled neurons encountered in the NTS and VLM. D. Of all the neurons double-labeled for FG and c-Fos following LPS treatment, the majority in the NTS (77%) and virtually all in the VLM (99%) are also labeled for DBH immunoreactivity.
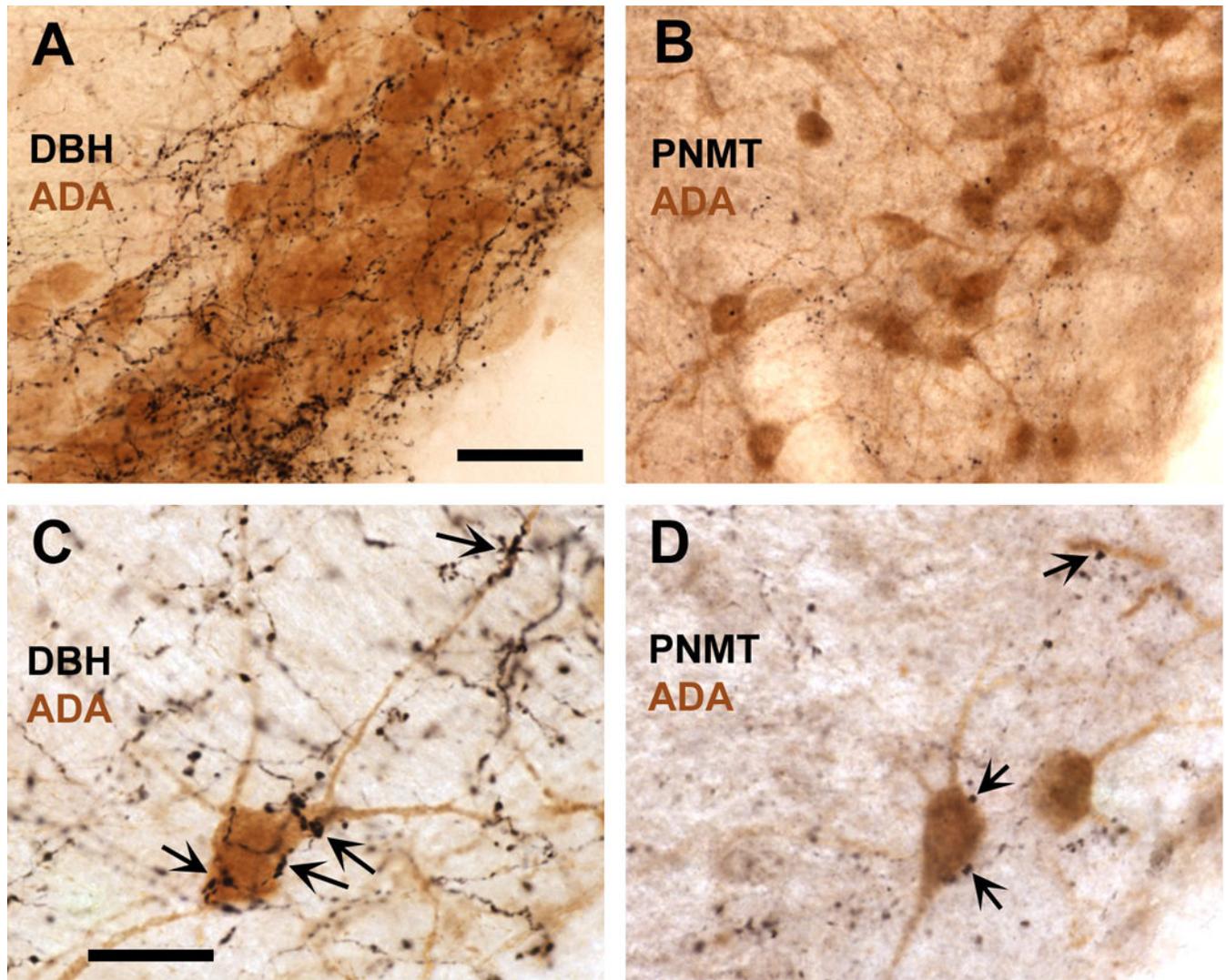
Fig. 10.
Rich catecholaminergic innervation in the histaminergic cell-rich ventral tuberomammillary nucleus as demonstrated by the dense plexus of DBH-immunoreactive varicose fibers (black) intermingling with adenosine deaminase (ADA)-positive cells (brown), a marker for histaminergic neurons in the VTM (A). Although considerably less dense, the VTM is also supplied by rather fine PNMT-positive fibers, vaticosities and terminal boutons (B), indicative of adrenergic innervation, which is exclusively derived from the medulla. Both the DBH- and PNMT-labeled fibers and varicosities are predominantly distributed amongst the ADA-positive cells in the VTM, and are much sparser in the adjacent portions of the ventral posterior hypothalamus. Photomicrographs taken under higher magnification reveal close appositions of DBH- and PNMT- labeled varicosities (C and D, respectively) with ADA-immunreactive cell bodies and dendrites, indicative of a direct catecholaminergic influence on these cells. Scale bar in A = 50 µm, also applies to B; scale bar in C = 25 µm, also applies to D.
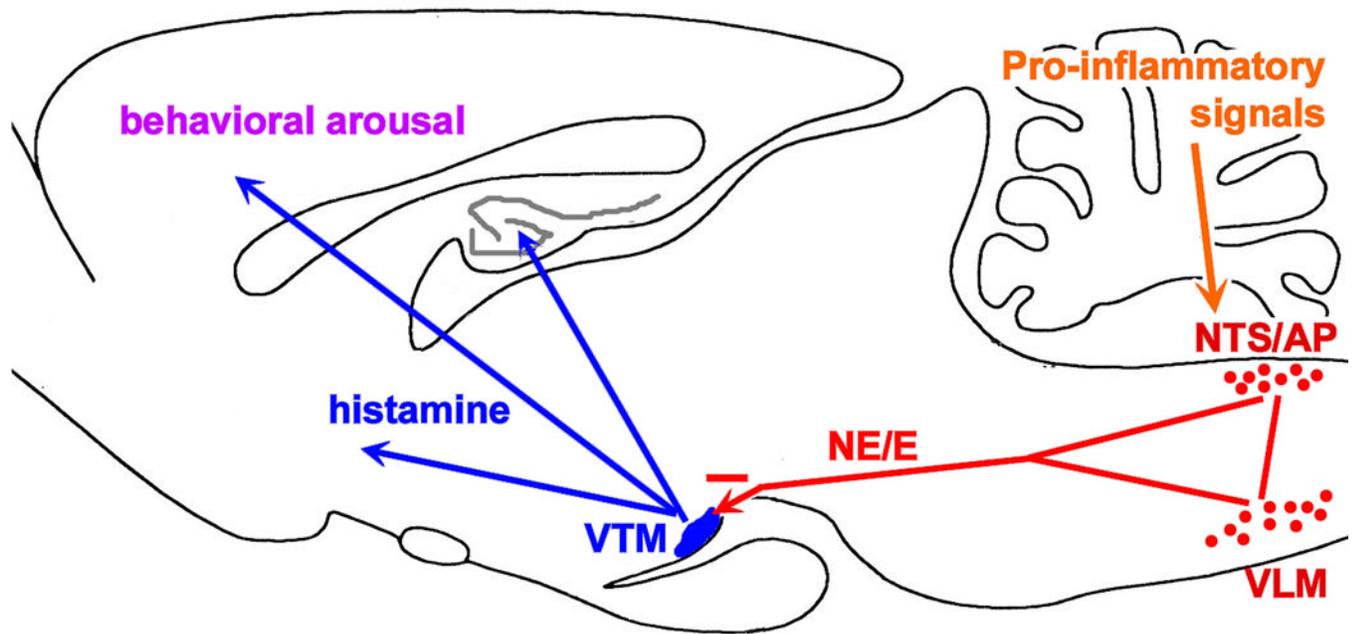
Fig. 11.
Summary model based on the present findings. The brain diagram depicting the inhibitory, primarily catecholaminergic influence, arising from the NTS and VLM, on the histaminergic system in the ventral tuberomammillary nucleus (VTM) of the hypothalamus. This inhibitory influence is initiated by a peripheral inflammatory stimulus (like LPS), and result in diminished behavioral arousal, a process highly dependent on activation of the histaminergic system.